

# Nonlinear photoelectric emission from metals induced by a laser radiation

S. I. Anisimov

*L. D. Landau Institute of Theoretical Physics, USSR Academy of Sciences, Moscow*

V. A. Benderskii

*Institute of Chemical Physics, USSR Academy of Sciences, Chernogolovka (Moscow Province)*

G. Farkas

*Central Institute of Physics Research, Hungarian Academy of Sciences, Budapest*  
*Usp. Fiz. Nauk 122, 185-222 (June 1977)*

A review is made of the current status of research on the nonlinear photoelectric emission resulting from the action of high-power laser radiation. The main experimental results are considered and possible theoretical interpretations are discussed. Considerable attention is concentrated on topics investigated recently, such as photoelectric emission in electrolyte solutions; photoelectric emission under the action of ultrashort laser pulses; detailed time, polarization, energy, and some other characteristics of photoelectric emission. Methods and results of calculations of the nonlinear photocurrent from the surfaces of metals are described. Theoretical results obtained by various methods are compared with one another and with the experimental data.

PACS numbers: 79.60.Cn

## CONTENTS

1. Introduction . . . . .	467
2. Experimental Investigations of Nonlinear Photoelectric Emission from Metals in Vacuum Caused by Nanosecond Laser Pulses . . . . .	468
3. Experimental Investigations of Nonlinear Photoelectric Emission from Metals in Electrolyte Solutions . . . . .	473
4. Experimental Investigations of Electron Emission from Metals in Vacuum Caused by Picosecond Laser Pulses . . . . .	476
5. Theory of Nonlinear Photoelectric Effect . . . . .	481
Literature . . . . .	487

## 1. INTRODUCTION

Extensive use of lasers in various branches of experimental physics began in the Sixties and has opened up new opportunities to solve a number of fundamental problems. It is sufficient to mention here investigations of many-photon processes in atoms and molecules,<sup>[1]</sup> new ideas on controlled thermonuclear fusion,<sup>[2-4]</sup> laser isotope separation methods,<sup>[5,6]</sup> and laser methods for investigations in solid-state physics.<sup>[7-9]</sup> Among the latter applications there is a considerable interest in studies of many-photon processes in solids and particularly in the nonlinear photoelectric emission. The current status of research on this effect is reviewed below.

The first estimates of the efficiency of electron emission from a metal as a result of the absorption of two photons were published well before the discovery of the laser.<sup>[10]</sup> However, the opportunity to observe experimentally this two-photon effect had to await the development of sufficiently powerful lasers. It was found that, in addition to the high illumination intensity, two-photon emission requires a suitable experimental method which makes it possible to eliminate the emission currents due to other mechanisms. The first report<sup>[11]</sup> of a photocurrent proportional to the square of the light intensity was published in 1964. The method used in that investi-

gation was unsuitable for the observation of processes of higher orders in intensity. A much more effective method was the one proposed by Farkas *et al.*,<sup>[12]</sup> which made it possible to study photoelectric emission as a result of the absorption of three or more photons. The experimental results were found to be in a satisfactory agreement with the first theoretical calculations of the probability of the many-photon photoelectric emission.<sup>[13-15]</sup> Somewhat later measurements of the absolute values of the quantum efficiency of the two- and three-photon processes<sup>[16]</sup> also confirmed the qualitative correctness of the theoretical calculations.

The cited investigations were typical of the first stage of the research on the many-photon photoelectric effect. At that stage the main problem was to observe the effect and no attempt was made to carry out detailed investigations of such important characteristics as the angular and energy distributions of the emitted photons, or the time, spectral, threshold, and polarization dependences of the photocurrent. A comparison of the theoretical and experimental results was limited basically to the lux-ampere characteristics and absolute values of the photocurrent. A fairly detailed review of the investigations carried out during this initial stage can be found elsewhere.<sup>[9,17,18]</sup>

We shall concentrate our attention on the investigations carried out recently and containing, in particular, analyses of the above-mentioned characteristics of the emission current. Although such investigations are of self-evident interest and—as demonstrated by studies of the conventional one-photon effect<sup>[19]</sup>—can give important information on the structure, electron spectra, and properties of the surface layers of solids, the corresponding experiments in the many-photon case are fairly difficult. One of the problems in quantitative experiments is the low value of the photocurrent and the related need to use high-power laser pulses. The practically unavoidable heating of the photocathode, which occurs under these conditions, gives rise to thermionic emission and masks the fine details of the photoelectric effect. An analysis shows that the thermal effects interfere with the observations of the photoelectric emission of sufficiently high order. The competition between the photoelectric and thermionic emission was first discussed by Bunkin and Prokhorov.<sup>[20]</sup> However, a complete analysis was given later<sup>[21,22]</sup> and was not included in the published reviews. The design and results of experiments on many-photon emission in vacuum, together with a qualitative analysis of the conditions for the observation of the photoelectric effect against the thermionic emission background, are given in Sec. 2.

A very interesting aspect of the investigations which are being pursued vigorously in recent years is the photoelectric effect in very strong electric fields. The theory predicts then a dependence of the emission current on the field of the same kind as for the field-electron emission.<sup>[15,23,24]</sup> Experimental studies of this case require suppression of the thermal effects and this can largely be achieved by employing ultrashort laser pulses. The first experiments of this kind were carried out using a train of picosecond pulses.<sup>[25,26]</sup> In these and later investigations a detailed study was made of the lux-ampere characteristics at incident light intensities up to tens of gigawatts per square centimeter. Considerable deviations were found from the standard power law valid at moderate intensities. The problem of interpretation of these deviations was found to be fairly complex; we shall discuss it in Sec. 5.

Another interesting problem also hardly touched upon in the published reviews is the many-photon emission of electrons at metal-electrolyte interfaces. This approach makes it possible to vary the work function within wide limits without altering other experimental parameters. This provides favorable conditions for the testing of the existing theoretical ideas on the photoelectric emission mechanisms. A detailed description of the experimental studies of many-photon emission in electrolytes and an analysis of the experimental results can be found in Sec. 3.

We shall not consider a number of important topics because this would have prevented a detailed treatment of the other topics. The omitted aspects include particularly the statistical characteristics of the nonlinear photoelectric emission and various considerations relating to the practical applications of the nonlinear photoelectric effect.

Some information on these subjects will be found in a review by Barashev.<sup>[9]</sup>

## 2. EXPERIMENTAL INVESTIGATIONS OF NONLINEAR PHOTOELECTRIC EMISSION FROM METALS IN VACUUM CAUSED BY NANOSECOND LASER PULSES

The first experimental investigations carried out in 1963–1965<sup>[27–30]</sup> were concerned with the emission of electrons from metal target surfaces illuminated with pulses generated in lasers operating in the free-oscillation regime so that the pulse duration was  $\sim 1 \mu\text{sec}$  and the average power was  $\sim 10 \text{ kW}$ ; such pulses consisted of trains of random irregular spikes. Electron emission was attributed to the optical heating of the target and quantitative results were not obtained because of the spiky nature of the pulses. Quantitative measurements required pulses with thoroughly investigated time and spectral characteristics, controlled distributions of the radiation intensity across the beam, and controlled peak intensity. Such pulses, frequently called giant pulses, can be obtained from Q-switched lasers. The shape of these pulses is nearly Gaussian and their half-width is  $\sim 10^{-8} \text{ sec}$  with a peak power density typically  $10^8 \text{ W/cm}^2$ . Ruby laser pulses with these characteristics were used in the first investigations carried out by Ready,<sup>[31]</sup> who measured the current from the surfaces of tungsten targets and concluded that the effect was of thermionic nature. Somewhat later, Knecht<sup>[32]</sup> obtained under similar experimental conditions some results which could not be explained entirely by the target heating.

Further systematic measurements of the electron emission were influenced strongly by the results of a theoretical investigation of the many-photon photoelectric effect. The theoretical analysis established the conditions under which many-photon emission can be identified reliably by experimental means. We shall first consider the characteristic features which distinguish photoelectric from thermionic emission.

a) In contrast to the thermionic current, the photocurrent is proportional to the  $n$ th power of the light intensity,

$$j_n = \eta_n I^n. \quad (1)$$

where  $\eta_n$  is the probability of the  $n$ -photon effect. The order  $n$  of the photoelectric effect can be deduced from the experimental data and compared with the theoretical value

$$n = \left\langle 1 + \frac{A}{\hbar\omega} \right\rangle,$$

where  $A$  is the work function for emission from a metal and the angular brackets  $\langle x \rangle$  denote the integral part of a number  $x$ . The agreement between the expected value of  $n$  and that found experimentally can be regarded as important evidence in support of the photoelectric nature of the measured current.

b) Since in the photoelectric effect the emission of electrons as a result of incidence of photons on the cath-

ode is an instantaneous process, the current pulse shows no delay relative to the laser pulse. However, because of the nonlinearity of the lux-ampere characteristic, the photocurrent pulse should be shorter than the laser pulse. For example, in the case of a Gaussian profile of the laser pulse the duration  $t_j$  of the photocurrent pulse is related to the laser pulse duration  $t_0$  by

$$t_j = \frac{t_0}{\sqrt{n}}.$$

In the thermionic emission case the shape of a current pulse is governed by the time dependence of the target temperature. The maximum of the current pulse is delayed relative to the laser pulse, its duration exceeds  $t_0$ , and the form of the decay is governed by the thermal properties of the target material (see the results in Refs. 8 and 30).

c) It is well known that the surface photoelectric effect is a typical vector phenomenon. The value of the current is governed by that component of the electric field of the incident wave which is normal to the surface and it depends strongly on the angle of incidence and on the polarization of light. In many-photon emission this dependence is very strong:

$$j_n \propto \xi^{2n} \propto \sin^{2n} \theta \sin^{2n} \varphi,$$

where  $\theta$  is the angle of incidence and  $\varphi$  is the angle of the plane of polarization relative to the plane of incidence. In the bulk photoelectric effect the dependence of the photocurrent on the angles of incidence and polarization is related to  $P^n$ , where  $P$  is the power absorbed in the metal but it differs slightly from this power law (this point is discussed in Sec. 5 below). On the other hand, the thermionic emission current is governed entirely by the temperature of the metal surface, which—in its turn—depends on the absorbed power. Thus, measurements of the angular and polarization dependences of the emission current make it possible to distinguish the many-photon surface photoelectric effect from the bulk effect, and the latter from thermionic emission.

d) The energy distribution of the electrons emitted as a result of the photoelectric effect differs greatly from the Maxwellian distribution found in the thermionic case. In the former case, the maximum of this distribution is close to the highest energy of the emitted electrons

$$E_{\text{max}} = n\hbar\omega - A$$

and is independent of the intensity of light and time, whereas in the latter case it is proportional to the target temperature and it varies with time.

These differences between the properties of the many-photon and thermionic emission currents make it possible, in principle, to observe the nonlinear photoelectric effect against the thermionic emission background. The suppression of the thermionic emission needed in quantitative measurements can be achieved by various methods. We shall now consider those which are used most frequently.

1) The thermionic current can be reduced by lowering

the laser beam intensity. However, the photocurrent—which is proportional to the  $n$ th power of the intensity—is then very low and this makes the measurements difficult. In practice, this method can be used only in investigating the two-photon effect and the experimentally determined current then includes a certain contribution of the one-photon process which is due to the thermal tail in the Fermi distribution.<sup>[11]</sup> We shall consider this problem in greater detail. The various contributions to the emission current are shown in Fig. 1. In the one-photon emission case in vacuum when  $kT \ll A - \hbar\omega$ , we have

$$j_1 = 2\eta_1 \left( \frac{kT}{A - \hbar\omega} \right)^2 \exp \left( \frac{\hbar\omega - A}{kT} \right), \quad (2)$$

where  $\eta_1$  is the quantum efficiency of the one-photon process. For constant laser intensity, the target surface temperature does not exceed

$$T_{\text{max}} = bIV\bar{t}_0, \quad b = \frac{1-R}{\sqrt{\pi\chi c\rho}}, \quad (3)$$

where  $c$ ,  $\chi$ , and  $\rho$  are, respectively, the specific heat, thermal conductivity, and density of the metal;  $R$  is the reflection coefficient of the surface. Figure 2 shows the calculated, on the basis of Eqs. (2) and (3), lux-ampere characteristics of the one-photon current associated with the Fermi distribution tail; the curves are plotted for various values of  $A - \hbar\omega$ . The calculations are carried out for typical parameters of metals:  $\eta_1 = 2 \times 10^{-4}$  A/W,  $b = 0.3$  deg·cm<sup>2</sup>·W<sup>-1</sup>·sec<sup>-1/2</sup>, and  $t_0 = 10$  nsec. We can easily see that the contribution of  $j_1$  falls exponentially with rising value of  $A - \hbar\omega$  and the lux-ampere characteristic is superlinear because of the temperature rise. If we then calculate the two-photon emission current and find the ratio  $j_2/j_1$ , we can show that the range of intensities where  $j_2 > j_1$  has upper and lower limits. This range decreases with decreasing  $A - \hbar\omega$  and it is practically impossible to observe the two-photon effect if  $A - \hbar\omega \lesssim 0.3$  eV. A rigorous calculation of the photocurrents of higher orders allowing for the target heating (Sec. 5) shows that even under optimal conditions it is practically impossible to observe currents with  $n > 6$  because of the thermal effects.

2) The thermionic current can also be reduced by reducing the power absorbed by the cathode when the angles of incidence are close to 90°. In this case the reflectivity of a plane metal surface is very high and for metals such as gold and silver it can reach 98–99%. This method makes it possible to reduce considerably the cathode heating and thus ensures the possibility of observing the nonlinear surface photoelectric effect which is due to the normal (to the metal surface) component of the electric field in the incident wave.

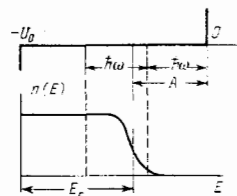


FIG. 1. Electron emission from a metal due to absorption of one and two photons.

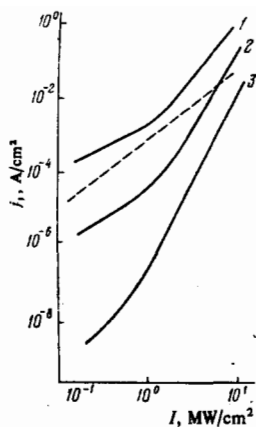


FIG. 2. Lux-ampere characteristics of the one-photon effect plotted for different values of  $A - \hbar\omega$  (eV): 1) 0.42; 2) 0.32; 3) 0.22. The dashed line shows the characteristic of the two-photon effect.

3) For a given laser radiation intensity the target temperature can be lowered by reducing the laser pulse duration. This possibility, proposed in Ref. 20, reduces in practice to the use (instead of the conventional giant pulses of about 10 nsec duration) of ultrashort pulses of about 10 psec duration generated in the self-mode-locked regime. When the laser pulses are of these very short durations, it is possible to avoid significant heating of the target even when the laser intensity is fairly high. However, the reduction in the pulse duration alters the nature of heating of the metal surface because there is no longer an equilibrium between electrons and the lattice and this affects the thermionic emission current<sup>[21]</sup> (see Sec. 4 below).

The apparatus used in studies of many-photon emission is basically similar for nanosecond and picosecond pulses and it consists of the following main parts (Fig. 5):

- a) a laser;
- b) elements for altering the intensity, polarization, and focusing of the laser beam (these are filters, polarizers, and prisms);
- c) elements for measuring the intensity, duration, and spatial distribution of the energy in a laser beam (these include fast linear photocells, calorimeters, high-speed cine cameras, and persistent-image oscilloscopes);
- d) a vacuum chamber with a metal target, a collector electrode (sometimes replaced with an electron multiplier), and a system for analysis of the energy distribution of the emitted electrons;
- e) instruments for recording the photocurrent pulses (wide-band amplifiers, pulse voltmeters, and fast-response oscilloscopes with a band of about 100 MHz for the nanosecond range).

We shall begin the review with the experimental results of the first study<sup>[11]</sup> which was intermediate between the preliminary measurements mentioned above<sup>[27-31]</sup> and subsequent systematic experiments involving nanosecond pulses. Teich *et al.*<sup>[11]</sup> investigated the emission from evaporated sodium films ( $A = 1.95$  eV) illuminated with gallium arsenide laser pulses of  $\lambda = 8400 \text{ \AA}$  wavelength, which were of about 3  $\mu\text{sec}$  duration and had a repetition frequency of 2.2 kHz. Since

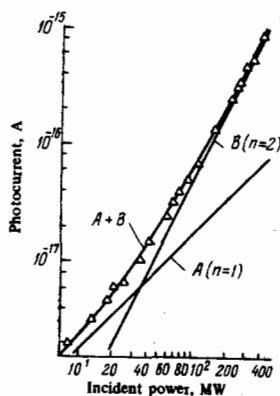


FIG. 3. Lux-ampere characteristic.<sup>[11]</sup>

the photon energy was 1.48 eV, two-photon emission was expected. Focusing on the target surface produced a power density up to  $10 \text{ kW/cm}^2$ . The lux-ampere characteristic obtained in this way is shown in Fig. 3. It can be represented by a sum of linear ( $A$ ) and quadratic ( $B$ ) components of the photocurrent. The linear component is due to the one-photon emission from the tail of the energy distribution. The experimentally determined rise of the photocathode temperature did not exceed  $2^\circ\text{C}$ , which indicated the absence of the thermionic current. In accordance with the above analysis, the contribution of the two-photon emission increased with the illumination intensity. The measured currents were extremely small: from  $6 \times 10^{-18}$  to  $3 \times 10^{-16}$  A.

The experimental values of the two-photon current agreed, to within a factor of 3, with the calculations of Smith<sup>[13]</sup> but his results were modified later.<sup>[33]</sup> One should also note that Teich *et al.*<sup>[11]</sup> first attributed their data to the surface photoelectric effect although the current was observed for normal incidence of light on the photocathode, when (for self-evident reasons) there should be no surface effect. In a later investigation the same authors<sup>[34]</sup> considered the two-photon emission from sodium under the action of helium-neon and gallium arsenide laser radiations as the bulk effect. In Ref. 35 the two-photon emission was measured in the absence of the thermal background. However, the experimental value of the quantum efficiency of the two-photon effect was three orders of magnitude higher than that predicted by the theory.<sup>[36]</sup>

We shall now consider the results obtained using nanosecond laser pulses. In the experiments described be-

TABLE I.

Laser	Wave-length, $\mu$	Photon energy, eV	Pulse duration, nsec	Power, MW
Ruby	0.6943	1.78	25	10-100
Ruby, second harmonic	0.3471	3.57	25	10-50
Neodymium glass	1.06	1.17	40	10-100
Neodymium glass, second harmonic	0.53	2.34	40	10-50

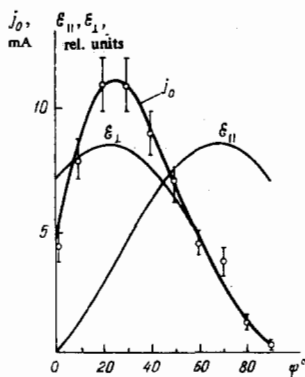


FIG. 4. Dependence of the photocurrent on the polarization of the incident radiation.

low the light sources were ruby and neodymium glass lasers. The pulses usually had Gaussian time and frequency profiles and were of about 10 nsec duration. In some cases the frequency was doubled in KDP crystals. The pulse characteristics are listed in Table I.

### A. Polarization dependence of photocurrent

Farkas *et al.*<sup>[12]</sup> used a ruby laser and a silver photocathode with a work function of 4.7 eV. A laser beam passed through a Glan-Thompson prism and fell on the cathode surface at an angle of 87°. Rotation of the prism altered continuously the parallel and perpendicular (to the surface) components of the electric field of the incident wave. The results obtained are plotted in Fig. 4. We can see that only the component of the field perpendicular to the cathode surface is important in the emission process and the emission current depends strongly on the polarization of the incident radiation. The duration of the photocurrent pulses is less than the duration of the laser pulses, which indicates that the process is of many-photon nature.

It is interesting to note that the one-photon effect in silver at the same maximum electron energy (about 0.5 eV) is interpreted in Ref. 37 as the bulk effect, whereas the three-photon effect is, according to Ref. 12, a pure surface phenomenon.

### B. Dependence of photocurrent on radiation intensity

The theory of the nonlinear photoelectric effect predicts that the emission current should depend on the light intensity in accordance with Eq. (1), which is valid

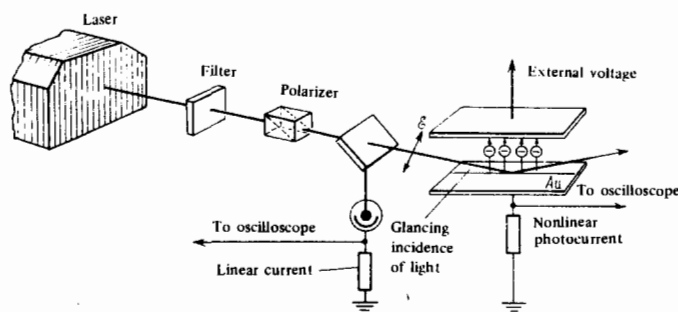


FIG. 5. Schematic diagram of the apparatus for the observation of nonlinear photoelectric emission in vacuum.

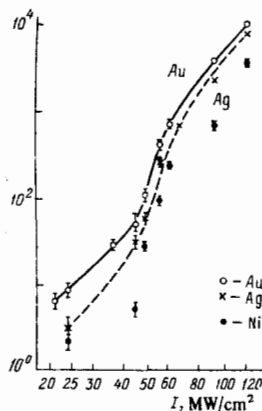


FIG. 6. Dependence of the photocurrent on the illumination intensity.<sup>12</sup>

for moderately high intensities. Experimental investigations of this dependence were carried out almost simultaneously.<sup>[38, 39]</sup> Later<sup>[34, 40]</sup> more detailed measurements were carried out.

In the investigation reported in Ref. 38 an unfocused ruby laser beam was directed onto a cathode almost parallel to its surface. The beam intensity was varied from 24 to 120 MW/cm<sup>2</sup>, which corresponded to a power density on the target from 2 to 10 MW/cm<sup>2</sup>. The cathodes were made of gold, silver, or nickel and their work functions were 4.8 eV, 4.8 eV, and 5.1 eV, respectively. The order of the photoelectric effect was 3. The results of the measurements are plotted in Fig. 6, which shows that the dependence  $j_3 \propto I^3$  applies to gold and silver in the range from 2 to 5 MW/cm<sup>2</sup>. At higher intensities the dependence becomes steeper, which may be attributed to the target heating. In the case of the nickel cathode the experimental data are subject to a large scatter because of the poorer optical and thermal properties of nickel.

In the study reported in Ref. 39 the light source was a ruby laser emitting pulses of 1 J energy and 40 nsec duration. An unfocused beam fell at an angle of 60° on a cathode which was a thin gold film on a steel substrate. The three-photon emission was observed at intensities below 1 MW/cm<sup>2</sup>; a further increase in the intensity resulted in a rapid rise of the current because of the thermal effects (Fig. 7). The intensity at which the thermionic emission became important was lower than in Ref. 38 because in Ref. 39 the angle of incidence was less and the absorbed power and cathode temperature were higher than in Ref. 38. The investigation reported in Ref. 39 yielded the constant  $\eta_3$  in the relationship  $j_3 = \eta_3 I^3$ . This constant was  $\eta_3 = 1.0 \times 10^{-3} \text{ A} \cdot \text{cm}^4 \cdot \text{MW}^{-3}$ . The quantum efficiency, defined as the number of photoelectrons emitted as a result of incidence of one photon, was thus found to be  $1.8 \times 10^{-25} I^2$ .

In the second part of the investigation reported in Ref. 39 the authors studied the two-photon effect using the same target and the second harmonic of a ruby laser ( $A = 4.8 \text{ eV}$ ,  $2\hbar\omega = 3.57 \text{ eV}$ ). At intensities below 1 MW/cm<sup>2</sup> the observed current was entirely due to the two-photon effect (Fig. 8). The measured value of the constant in the expression for the emission current  $j_2 = \eta_2 I^2$  was  $2.35 \times 10^{-15} \text{ A} \cdot \text{cm}^2 \cdot \text{W}^{-2}$ . The dependence of the

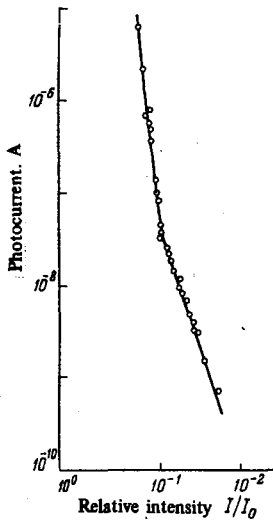


FIG. 7. Lux-ampere characteristic in the region of transition from photoelectric to thermionic emission ( $I_0 = 14 \text{ MW/cm}^2$ ).

quantum efficiency of the effect on the intensity is also shown in Fig. 8.

In a later investigation<sup>[16]</sup> the same authors were concerned with details of the nonlinear photoelectric emission from the surfaces of various metals, including stainless steel ( $A = 5.0 \text{ eV}$ ). They expected photocurrents with  $n = 3-4$  for ruby laser radiation and with  $n = 5$  for neodymium laser radiation. Instead, in both cases they observed a poorly reproducible dependence of the type (1) with  $n \approx 7$  and this was evidently due to the thermal effects. For the second harmonic of a ruby laser they observed the theoretically expected two-photon emission in the range of intensities from  $1 \text{ kW/cm}^2$  to  $1 \text{ MW/cm}^2$ .

Thus, an analysis of these investigations shows that the nonlinear photoelectric effect as a result of nanosecond laser pulses can be observed only in a limited range of radiation intensities from about  $10 \text{ kW/cm}^2$  to  $1-5 \text{ MW/cm}^2$ ; moreover, it is impossible to observe photocurrents of order higher than the third because of the thermal effects, the main of which is the emission of lower orders because of transitions from the energy distribution tail. We shall show later (Sec. 4) that this range can be extended by the use of picosecond pulses.

### C. Time characteristics of emission current

The time characteristics of the emission current were reported in Ref. 40. A ruby laser pulse of Gaussian

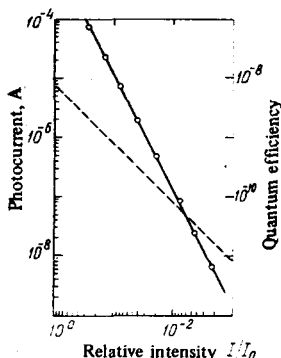


FIG. 8. Quantum efficiency of the two-photon effect ( $I_0 \approx 1 \text{ MW/cm}^2$ ).

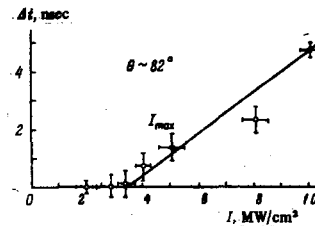


FIG. 9. Delay of the emission current relative to the laser pulse.

profile and  $20 \text{ nsec}$  half-width was directed on an Au cathode at an angle of  $82^\circ$ . The time interval between the laser pulse maximum and the emission current maximum was determined as a function of the laser intensity. The results are plotted in Fig. 9. We can see that at intensities below  $4 \text{ MW/cm}^2$  there is no delay, which indicates that the current pulses are due to the photoelectric effect. Above  $4 \text{ MW/cm}^2$ , there is a delay in the emission current and this is in agreement with the lux-ampere characteristics described above.

An additional confirmation of the results obtained was provided by the measurements of the half-width of the emission current pulses. When the half-width of the laser pulses was  $40 \text{ nsec}$ , the half-width of the current pulses reported in Ref. 16 was  $22 \text{ nsec}$ , which was exactly the value expected for the three-photon effect. The half-width of the current pulses was determined in Ref. 40 as a function of the light intensity (Fig. 10). As expected, at intensities in the range  $I < 4 \text{ MW/cm}^2$  the half-width of the current pulse was  $20/\sqrt{3} = 11 \text{ nsec}$ ; at higher intensities this half-width increased indicating predominance of thermionic emission.

### D. Energy distribution of emitted electrons

An experimental investigation of the energy distribution of the emitted electrons was reported in Ref. 16. When iron and gold targets were illuminated with ruby laser radiation, the energy distribution maximum was located at zero energy (Fig. 11), which corresponded to thermionic emission. In the case of the second harmonic of the same laser radiation the distribution function of the emitted electrons had a maximum located at about  $1 \text{ eV}$ , which indicated that the emission was now of many-photon nature. In comparisons of the experimental and theoretical results it would undoubtedly be of interest to determine the dependence of the photocurrent on the electron energy. This dependence could, in principle, be found by analyzing the energy distribution of the emitted electrons. However, in practice the precision of the measurement reported in Ref. 16 was sufficient only to distinguish the photocurrent from the current due to thermal effects.

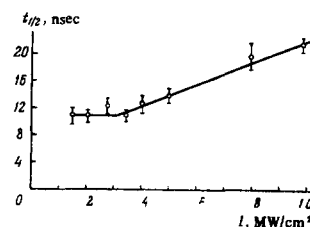


FIG. 10. Dependence of the half-width of the current pulse on the laser radiation intensity. The half-width of the laser pulse was  $20 \text{ nsec}$ .

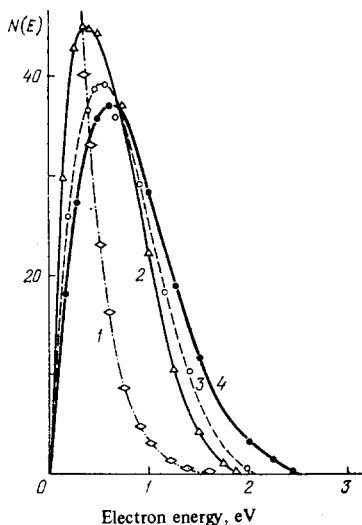


FIG. 11. Energy distribution of the emitted electrons; 1) thermionic emission; 2)–4) photoemission due to second harmonic of ruby laser incident on steel (2), Ag (3), and Au (4).

The dependence of the photocurrent on the frequency of the incident radiation is also of considerable interest. The difficulty in these measurements is the fact that the photocurrent is usually determined at the fixed frequency of a given laser. Spectral measurements of many-photon emission in vacuum are fraught with considerable methodological difficulties and have not yet been carried out. Some of the difficulties in the experimental determination of the dependence of the photocurrent on the frequency of the incident radiation and the energy of the emitted electrons can be overcome by investigating nonlinear photoelectric emission from various targets in electrolyte solutions. In this case there is no need to carry out spectral measurements because the work function can be varied by altering the photocathode potential. The results of such experiments are considered in the next section.

### 3. EXPERIMENTAL INVESTIGATIONS OF NONLINEAR PHOTOELECTRIC EMISSION FROM METALS IN ELECTROLYTE SOLUTIONS

The difference between the photoemission from metals in electrolyte solutions and the emission in vacuum is due to, firstly, the potential drop in a double electric layer at the metal–electrolyte interface (the thickness of this layer is much less than the wavelength of the emitted electrons) and, secondly, due to the Coulomb screening in the solutions, which weakens the electric image forces. The first difference makes the red edge of the photoelectric effect a linear function of the potential

$$\hbar\omega = \hbar\omega_0 - e\varphi,$$

where  $\hbar\omega_0$  is the work function of a metal in a solution in the absence of any charge on the interface and  $\varphi$  is the photocathode potential, measured from the zero-charge point. The Coulomb screening makes the dependence of the photocurrent on the maximum energy of the emitted electrons obey the “five-halves” law and not the usual Fowler law. These features have been investi-

gated in detail in the one-photon effect.

The photoelectric emission from mercury into an electrolyte solution under the action of ruby and neodymium laser pulses was first observed by Korshunov *et al.*<sup>[42]</sup> They found that the current produced by spiky ruby laser pulses was a quadratic function of the illumination intensity, in agreement with the theoretically expected two-photon emission. The photocurrent-voltage characteristic obeyed, within the limits of the experimental error, the five-halves law. This confirmed the theoretically predicted dependence of the nonlinear photocurrent with  $n = 2$  on the energy of the emitted electrons which had not been established (as pointed out at the end of the preceding section) in studies of many-photon emission in vacuum.

Additional more detailed investigations of two-photon emission<sup>[43–45]</sup> were carried out using nanosecond laser pulses. Use was made of the apparatus shown schematically in Fig. 12. A laser pulse crossed a system of calibrated attenuators, mirrors, and filters before reaching the cathode of an electrochemical cell. Part of the laser beam, separated by quartz plate, was deflected to a microcalorimeter, which was used to measure the laser pulse energy, and to a fast-response photodiode, which determined the amplitude and shape of the laser pulses. The signal at the output of the electrochemical cell was amplified with a wide-band amplifier and recorded with a persistent-image oscillograph. The high capacitance of the electrochemical cell made it necessary to measure the emitted charge rather than the current.

In addition to the interference resulting from the thermal effects (discussed in the preceding section), the electrochemical cell suffered from heating when the illumination was strong. However, the total current produced by such secondary effects was zero provided the recording time was longer than the thermal relaxation time. When this condition was satisfied, the measured signal was proportional to the emitted charge. On the other hand, measurement of the heating signal enabled us to determine directly the electrode temperature.

The sensitivity of the recording apparatus in the charge measurement method was not sufficient to be

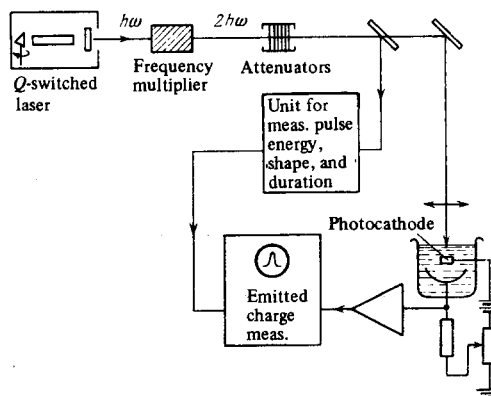


FIG. 12. Schematic diagram of the apparatus used in studies of nonlinear photoelectric emission in an electrolyte.



able to reduce the laser pulse duration because even for  $t_0 \sim 10^{-6}$  sec the many-photon emission signal was  $10^{-5}$ – $10^{-3}$  V and the signal could be isolated only by reducing the pass band of the measuring system which—like the presence of the heating signal—made it impossible to carry out measurements of the signal kinetics.

Since the conditions in measurements of the many-photon emission in vacuum and electrolyte solutions are clearly different (moreover, in the latter case one cannot measure the energy distribution of the emitted electrons), the photoelectric effect is identified on the basis of characteristics other than those listed at the beginning of Sec. 2. The new characteristics are:

- a) a power-law dependence of the emitted charge on the intensity of light;
- b) the five-halves law obeyed at all light intensities, which is equivalent to independence of the energy distribution of the emitted electrons from the illumination intensity;
- c) coincidence of the thresholds of the two- and one-photon emission effects (corresponding to identical extrapolation potentials of the current-voltage characteristics) in the case when the excitation is in the form of laser pulses carrying photons of energies  $\hbar\omega$  and  $2\hbar\omega$ , respectively;
- d) equality of the difference between the extrapolation potentials to the photon energy when the order of the photoelectric effect changes by unity.

The last two characteristics can be deduced directly from the dependence of the  $n$ -photon photocurrent on the maximum energy of the emitted electrons:

$$j_1 \sim (\hbar\omega - \hbar\omega_0 + e\varphi)^{5/2}, \quad e\varphi_{01} = \hbar(\omega_0 - \omega), \quad (4)$$

$$j_2 \sim (2\hbar\omega - \hbar\omega_0 + e\varphi)^{5/2}, \quad e\varphi_{02} = \hbar(\omega_0 - 2\omega). \quad (5)$$

Table II gives the values of the extrapolation potentials  $\varphi_{0n}$  for two- and one-photon emission under the action of the first and second harmonics of ruby and neodymium lasers.

It is clear from Table II that in the range of potentials of the mercury electrode (from +0.1 to -2.0 V relative to the saturated calomel electrode) photoelectric emission can be of the one- and two-photon type. Moreover, when the electrode potential is varied, the predicted change in the order of the photoelectric effect should be observed: the transition from  $n = 2$  to  $n = 1$  should take

TABLE II

Laser	Photon energy, eV	$\varphi_{01}$ , V*	$\varphi_{02}$ , V*
Ruby	1.78	-1.73	-0.06
Ruby, second harmonic	3.57	+0.06	...
Neodymium glass	1.17	-2.34	-1.17
Neodymium glass, second harmonic	2.34	-1.17	-1.17

\*) The values of the potentials are given relative to the saturated calomel electrode.

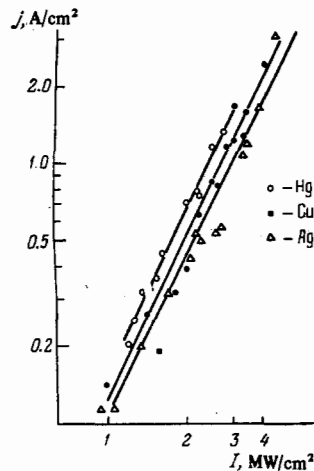


FIG. 13. Two-photon emission from Hg, Ag, and Cu.

place under the action of the first harmonic of ruby laser radiation and the second harmonic of neodymium laser radiation, which can be used to determine directly the ratio of the efficiencies of the photoelectric effects with  $n = 2$  and  $n = 1$ , provided it is possible to eliminate the changes in  $j_2/j_1$  due to different conditions in the absorption of light of different wavelengths in the metal and due to the difference between the characteristics of pulses emitted by different light sources, which have to be used in measurements of the photoelectric emission in vacuum.

We shall now present the experimental results. The quadratic dependence of the emitted charge on the intensity of nanosecond ruby laser pulses (30 nsec duration) was observed for mercury, lead, silver, and copper up to  $3 \text{ MW/cm}^2$  in the incident beam for angles of incidence of  $45^\circ$  on solid electrodes and from  $60^\circ$  to  $90^\circ$  on mercury. These dependences are plotted in Fig. 13 and they are taken from Ref. 43. The value of  $n$  found in this way is  $2 \pm 0.2$ . Figures 14 and 15 show the dependences  $Q(I)$  for one- and two-photon emission from mercury and lead under the action of, respectively, the second and first harmonics of a ruby laser.<sup>[45]</sup> An increase in the temperature of the metal under the influence of radiation of  $I = 3 \text{ MW/cm}^2$  intensity, estimated from the heating signal, did not exceed  $50^\circ \text{C}$ , in agreement with the calculations. The thermionic and photoelectric current from the energy distribution tail was 4–5 orders of magnitude less than the two-photon emission current (compare Figs. 2 and 3). A considerable

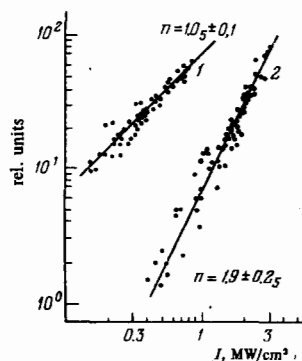


FIG. 14. Lux-ampere characteristics of one-photon (1) and two-photon (2) emission from Pb in an electrolyte solution.



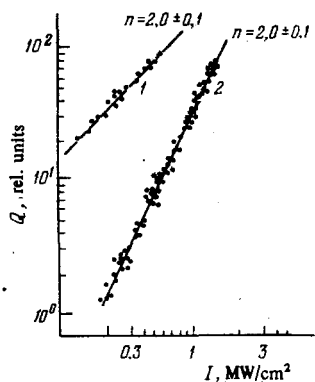


FIG. 15. Lux-ampere characteristics of one-photon (1) and two-photon (2) emission from Hg in an electrolyte solution.

contribution of the thermal effects, manifested by a steep rise of the slope of the lux-ampere characteristic, was usually observed at light intensities exceeding 5 MW/cm<sup>2</sup>. The quadratic dependence of the current on the light intensity was reported for a mercury electrode in Ref. 46. In comparing the value  $I_{\max} = 5$  MW/cm<sup>2</sup> with that given in the preceding section ( $\sim 1$  MW/cm<sup>2</sup>) one should bear in mind that the order of the photoelectric effect was different ( $n = 2$  in the case of emission in electrolytes and  $n = 3$  in the case of emission in vacuum) and—since the probability of photoelectric emission for the same values of  $I$  fell by several orders of magnitude when  $n$  increased by unity—the value of the maximum intensity at which a given current was due to the photoelectric effect increased on transition from  $n = 3$  to  $n = 2$ .

The five-halves law was satisfied by the two-photon emission throughout the investigated range of the quadratic dependence  $Q(I)$ .

Figures 16 and 17 show the dependences of the emitted charge on the potential for one- and two-photon emission from mercury and lead. The experimental data are in good agreement with Eqs. (4) and (5) and, following the theoretical predictions, the one- and two-photon emission thresholds agree at the photon energies  $2\hbar\omega$  and  $\hbar\omega$ . The relationship (5) for the two-photon emission was confirmed in Ref. 46.

The order of the photoelectric effect was reduced from  $n = 2$  to  $n = 1$  by a change in the electrode potential in the investigation cited earlier.<sup>[43]</sup> Figure 18, taken from that paper, shows the dependence  $Q(\varphi)$  which clearly consists of two sections corresponding to one- and two-photon emission. In the two-photon emission range ( $-0.5 > \varphi > -1.7$  V relative to the saturated calomel electrode) the emitted charge is proportional to the square of the intensity of illumination and for  $\varphi < -1.7$  V this dependence becomes linear. The difference between the extrapolation potentials of the corresponding parts of the dependence  $Q(\varphi)$  is 1.7–1.8 V, which is in agreement with the theoretical predictions [Eq. (5)] and agrees—within the limits of the experimental error—with the laser photon energy. The quantum efficiency of the linear photocurrent, found in the range  $\varphi < -1.7$  V, is  $(1-2) \times 10^{-4}$  electrons/photon at the maximum emitted electron energy  $E_m = 0.5$  eV, which is in agreement with the results of measurements carried out at low illumination intensities. The ratio  $j_2/j_1$  for the same values of  $E_m$  is  $(1-2) \times 10^{-3}$  when  $I = 1.5-2$  MW/cm<sup>2</sup>. The value of  $\eta_2$  found from these data for the two-photon emission from mercury in an electrolyte solution (allowance is made for the doubling of the photoemission current because of the chemical reduction of the captured product) is  $(1.5-0.7) \times 10^{-14}$  A · cm<sup>2</sup> · W<sup>-2</sup>.

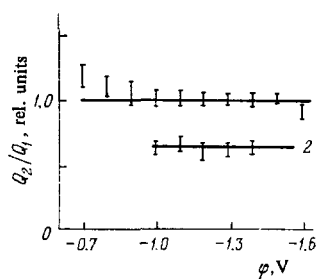


FIG. 17. Constancy of the ratio of the two- and one-photon emission signals plotted as a function of the electrode potential: 1) Pb; 2) Hg. Photoelectric emission with  $n = 1$  and 2 was excited by ruby laser radiation and its second harmonic, respectively.

The above change in the order of the photoelectric emission from mercury occurs also in the case of pulses of the second harmonic of neodymium laser radiation in the range of potentials identified in Table II.

In more accurate measurements of  $\eta_2$  a comparison was made of the charges emitted from the same metal target by pulses of the first and second harmonics of ruby laser radiation.<sup>[45]</sup> The values of  $\eta_2$  found in this way (Table III) were averaged over a considerable number of measurements carried out on different samples and could be regarded as correct to within a factor smaller than 2. Table III gives also the values of  $\eta_2$  deduced from measurements of the two-photon emission of electrons in vacuum.

It is clear from Table III that the values of  $\eta_2$  of dif-

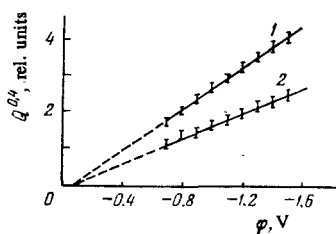


FIG. 16. Current-voltage characteristics of one-photon (1) and two-photon (2) emission from Pb in an electrolyte solution.

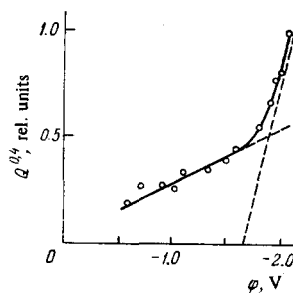


FIG. 18. Dependence of the order of the photoelectric effect on the electrode potential obtained for 0.01 M solution of  $(C_2H_5)_4Cl$  (ruby laser radiation of  $I = 2$  MW/cm<sup>2</sup> intensity).

TABLE III

Metal	Emission conditions	Photon energy, eV	Maximum electron energy, eV	$\eta_2$ $A \cdot cm^2 \cdot W^{-2}$	Reference
Sodium	Vacuum	1.48	0.7	$8 \cdot 10^{-16}$	34
"	"	1.96	1.6	$9 \cdot 10^{-16}$	35
Gold	"	3.57	2.3	$2.4 \cdot 10^{-15}$	19
Mercury	Electrolyte	1.78	1.2	$3.5 \cdot 10^{-14}$	45
Lead	"	1.78	1.1	$7.3 \cdot 10^{-14}$	45

ferent metals lie within the range  $10^{-15}$ – $10^{-13}$   $A \cdot cm^2 \cdot W^{-2}$ . The results for silver and copper<sup>[43]</sup> give  $\eta_2 \sim 10^{-14}$   $A \cdot cm^2 \cdot W^{-2}$  (see Fig. 13), which also lie in this range. In estimating the scatter of the values of  $\eta_2$  within two orders of magnitude we must bear in mind that the measurements on sodium films were carried out in  $10^{-6}$  Torr vacuum, which was insufficient to ensure a clean surface (see, for example, Refs. 48 and 49), and the values of  $\eta_2$  for gold, on the one hand, and mercury and lead, on the other, were obtained for photon energies differing by a factor of two and, in accordance with the theory,  $\eta_2$  should decrease rapidly with rising  $\omega$ . Such a variation was deduced also from the results of preliminary measurements described in Ref. 44, where a comparison was made of the probability of two-photon emission of electrons from mercury under the action of the first harmonics of ruby and neodymium laser pulses (in the latter case the emission occurred in the range  $\varphi < -1.5$  V relative to the saturated calomel electrode) and it was found that  $\eta_2$  in the second case was approximately an order of magnitude higher than in the first.

The angular dependence of the probability of two-photon emission from mercury ( $\hbar\omega = 1.78$  eV), determined in Ref. 44, is shown in Fig. 19. This figure includes also a similar dependence for the one-photon emission obtained at the same photon energy for the same sample. The latter agrees well with the angular dependence of the photocurrent at low illumination intensities.

#### 4. EXPERIMENTAL INVESTIGATIONS OF ELECTRON EMISSION FROM METALS IN VACUUM CAUSED BY PICOSECOND LASER PULSES

As pointed out in the Introduction, at very high (of the order of  $10$ – $100$   $GW/cm^2$ ) illumination intensities the nonlinear photoelectric effect exhibits a number of very interesting features. The well-known work of Keldysh<sup>[50]</sup> was followed by a series of theoretical papers<sup>[23, 24, 51–54]</sup> in which it was predicted that the usual power-law dependence of the emission current density on the laser intensity should break down at sufficiently high intensities. These investigations stimulated experimental studies of the photoelectric emission in strong optical fields.

Although intensities of the order of hundreds and thousands of gigawatts per square centimeter can readily be attained in nanosecond pulses, such pulses are unsuitable for the investigation of photoelectric emission in this range of intensities. In fact, as pointed out in Sec. 2, in the case of nanosecond pulses the range of reliable observation of many-photon emission has an upper intensity limit of the order of  $2$ – $5$   $MW/cm^2$ ; at

higher intensities the thermionic emission due to the cathode heating begins to make a considerable contribution to the observed current. Bunkin and Prokhorov<sup>[20]</sup> demonstrated that much more favorable conditions for studies of many-photon processes are established by reducing the laser pulse duration and at the same time increasing the illumination intensity. It was shown in Refs. 8 and 21 that heating of a metal with ultrashort pulses disturbs the equilibrium between electrons and the lattice and this should effect strongly the thermionic emission because of the low specific heat of the degenerate electron gas. A detailed calculation, which will be considered in greater detail in Sec. 5, showed that in the case of pulses shorter than  $10^{-11}$  sec the range of observation of the photoelectric effect against the thermionic emission background can be expanded to intensities of the order of  $10$ – $100$   $GW/cm^2$ .

The technique of generation of ultrashort laser pulses was developed in 1966–1967. The earliest information on the parameters of such pulses was obtained by the method of two-photon fluorescence. It was established that a self-mode-locked laser can emit a train of  $10$ – $100$  pulses of average duration of the order of  $10^{-12}$  sec, average power of the order of  $1$  GW, and an interval between the pulses  $\Delta t = 2L/c$ , where  $L$  is the length of the resonator and  $c$  is the velocity of light. Subsequently, electro-optic methods were used to isolate a single pulse from a train and to measure directly its duration by means of an image-converter camera.<sup>[55]</sup> These investigations established that during the first half of a train, when the intensity rises, each separate pulse is of Gaussian shape along the time and energy scales and has an average duration of about  $6$ – $7$  psec. During the second half of the train, when the intensity falls, the duration of the pulses increases to values of the order of  $100$  psec, and their profile and spectrum become irregular and acquire a substructure.

Before discussing the investigations of the nonlinear photoelectric effect under the action of picosecond pulses, we should note that measurements of photoelectric emission of higher orders can give useful information on the properties of the pulses themselves, particularly on their time structure, spectral characteristics, coherence, etc.

##### A. Dependence of photocurrent on radiation intensity

The first measurements of the lux-ampere characteristics of picosecond pulses were carried out in

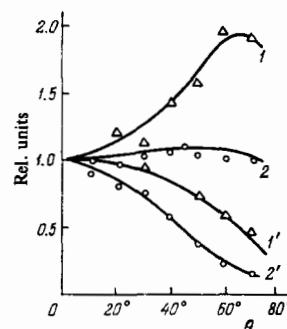


FIG. 19. Dependence of the emitted charge  $Q$  (rel. units) on the angle of incidence of polarized light: 1, 1') one-photon emission from Hg; 2, 2') two-photon emission from Hg; 1, 2)  $s$  polarization; 1', 2')  $p$  polarization. Ruby laser radiation,  $2$   $MW/cm^2$ .

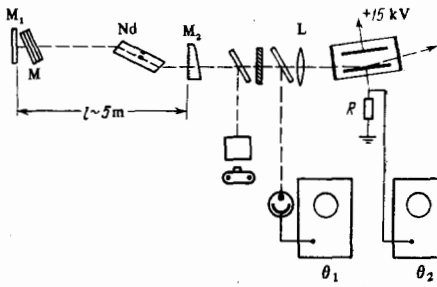


FIG. 20. Apparatus used in investigations of the photoelectric emission under the action of picosecond pulses.

1969.<sup>[56, 57]</sup> The apparatus used was described in Refs. 12 and 38 and it included a laser operated in the self-mode-locked regime. A train of picosecond pulses was recorded with two photoelectric detectors: a fast linear detector and a nonlinear one, in which a metal cathode was used. The signals from both detectors were applied to a fast-response oscillograph. Thus, the experiments yielded the averaged (over an interval governed by the oscillograph pass band, usually about 1 nsec) values of the linear and nonlinear currents, proportional to the integrals

$$V_L \sim \int I dt, \quad V_{NL} \sim \int I^n dt.$$

Clearly, only in the case when all the pulses in a train had the same time and spectral profiles could the intensity  $I$  be replaced with  $V_L$  and the current  $j \propto I^n$  with the value  $V_{NL}$ . The lux-ampere characteristic was obtained by plotting  $V_{NL}$  as a function of  $V_L$  on a double logarithmic scale.

The experiments<sup>[56, 57]</sup> revealed nonlinear photoelectric effects of different orders—from the second to the fifth—when the laser beam intensity was about  $1 \text{ GW/cm}^2$ . Exact absolute values of these intensities were not measured because at that time it was still difficult to determine the durations of ultrashort pulses. The apparatus employed was of the type shown schematically in Fig. 20. Ruby and neodymium glass lasers were used; the target materials were Au and Ni as well as the semiconductor  $\text{Cs}_3\text{Sb}$ . In the case of the neodymium laser radiation and the Au cathode small fluctuations of the work function would alter the expected value of  $n$  from 5 to 4. Therefore, in the case of polycrystalline samples either of these values could be obtained, depending on the structure of the sample.

It is clear from Fig. 21 that the experiments described above revealed the pure many-photon effect of the second, third, fourth, and fifth orders without a significant contribution of thermionic emission. The experimental error in the determination of  $n$  was  $\pm 0.5$ .<sup>1)</sup> The experiments indicated some increase of the current at the end of a pulse train, which was one of the first experimental indications of an increase in the duration of

<sup>1)</sup>In the case of a  $\text{Cs}_3\text{Sb}$  cathode, which is used as a control, the thermal effects become perceptible at lower intensities than in the case of metal cathodes because of the lower thermal conductivity of  $\text{Cs}_3\text{Sb}$ .

the individual pulses at the end of a train. Essentially, the main importance of the experiments reported in Refs. 56 and 57 was that they confirmed that the many-photon effect could be observed in the range of intensities  $\sim 1 \text{ GW/cm}^2$  or higher. This provided an opportunity for a detailed investigation of the characteristics of photoelectric emission in strong optical fields.

The theory of photoelectric and thermionic emission under the action of picosecond pulses is discussed in detail in Sec. 5. However, we must mention here two theoretical results which are essential for the understanding of the experiments described below. The first relates to the dependence of the photocurrent on the illumination intensity. We have seen above that at relatively low intensities the photocurrent is a power-law function of the illumination intensity. On the other hand, if the wave field intensity becomes so high that the probability of tunnel knocking out of an electron in one period is of the order of unity, the dependence of the emission current on the field intensity should reduce to the well-known expression for the field-electron emission in a static field. A similar situation applies naturally in the case of many-photon ionization of atoms.<sup>[1]</sup> A formula derived in Ref. 50 and valid in the limits of weak and strong fields applies specifically to this case. According to Refs. 15, 24, and 50, the critical field intensity is  $\mathcal{E}_* \sim (\omega/e)\sqrt{2}mA$ , where  $e$  and  $m$  are the electron mass and charge, and  $\omega$  is the radiation frequency. For a neodymium laser and a gold cathode an estimate gives a critical value of  $\mathcal{E}_* \sim 10^{7.3} \text{ V/cm}$ . This value is obtained without allowance for the Coulomb interaction between the emitted electron and the metal surface. Such allowance reduces the critical field by more than one order of magnitude.<sup>[23]</sup>

Secondly, as shown in Refs. 8 and 21, the nature of the thermionic emission changes greatly in the picosecond range of pulse durations. For these durations the

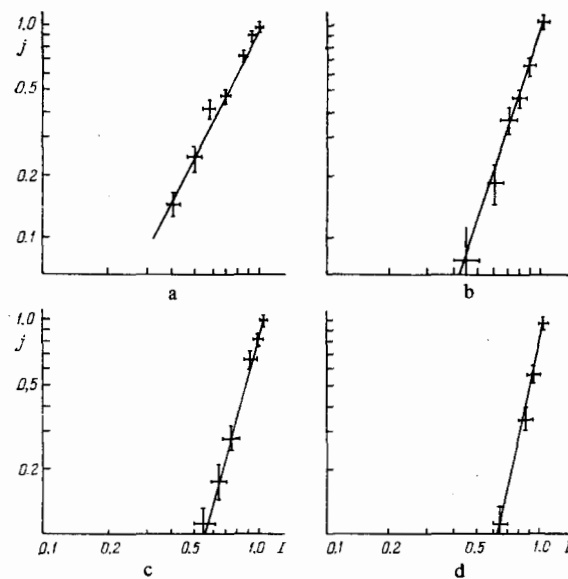


FIG. 21. Lux-ampere characteristics: a)  $\text{Cs}_3\text{Sb}$  cathode, neodymium laser,  $n=2$ ; b) Au, ruby laser,  $n=3$ ; c) Au, neodymium laser,  $n=4$ ; d) Ni, neodymium laser,  $n=5$ .

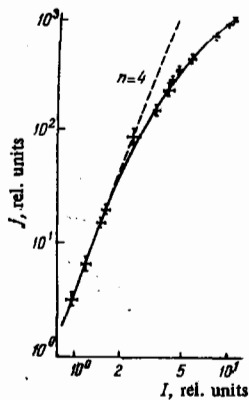


FIG. 22. Reduction in the degree of nonlinearity at high illumination intensities.

electron subsystem is isolated from the lattice and, because of its low specific heat, this subsystem is heated practically instantaneously. Consequently, when picosecond pulses are used, the thermionic emission current is not delayed relative to the laser pulse. In the simplest experiments it is difficult to separate such thermionic emission from photoelectric emission; the superposition of the two mechanisms results in a dependence of the current on the illumination intensity other than that given by Eq. (1).

An experimental check of these theoretical predictions was made in Ref. 58. An improved variant of the apparatus described in Ref. 57 was used. The results were analyzed by the same technique as in Ref. 57. Radiation emitted by a self-mode-locked neodymium laser was focused on the surface of a cathode. Measurements were carried out in the range of laser intensities from 6.5 to 66 GW/cm<sup>2</sup>. The relevant values of  $\xi_1$  range from 10<sup>6.3</sup> to 10<sup>6.8</sup> V/cm. The experimental results are plotted in Fig. 22. We can see that when the normal component of the field is  $\xi_1 \sim 10^{6.8}$  V/cm, there is a deviation from the usual power dependence of the emission current. However, the experimentally determined critical value of the field intensity, corresponding to the onset of this deviation, is slightly less than the theoretically predicted<sup>[24]</sup> value 10<sup>7.3</sup> V/cm. However, it should be pointed out that the accuracy of the absolute measurements of the field intensity was not very high because the two-photon fluorescence method gave the pulse durations averaged over a train. Moreover, the experiments indicated that the emission current and the random scatter of the results depended strongly on the parameters of the ultrashort pulses and their distribution in a train.

A more detailed investigation of the same topics was reported in Ref. 59. Use was made of the apparatus described in Ref. 58. Signals from a linear detector and a photocathode passed along a delay line and were

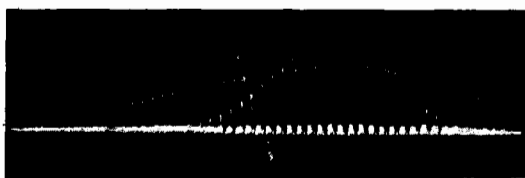


FIG. 23. Oscillograms of linear and nonlinear signals.

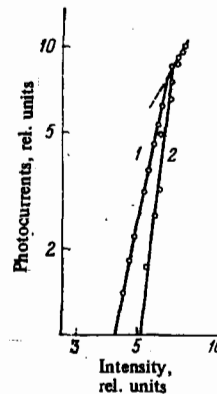


FIG. 24. Dependence of the photocurrent on the intensity of illumination provided by a laser emitting a train of picosecond pulses: 1) part of the train with rising intensity; 2) part of the train with falling intensity.

applied simultaneously to a fast-response oscillograph. The signals were trains of current pulses (Fig. 23). The duration of the signal from the nonlinear photocathode (measured along the envelope) was less than the duration of the linear signal. The lux-ampere characteristic based on Fig. 23 is plotted in Fig. 24. This characteristic has three different regions. The initial part of the train, when the intensity rises, corresponds to the straight line of slope 5, describing photoelectric emission due to the absorption of five photons. An increase in the maximum intensity reduces the slope in accordance with the theoretical predictions<sup>[24, 23, 50, 54]</sup> and the results reported in Ref. 58. Finally, the third part of the curve, corresponding to a part of the pulse train in which the intensity decreases, reveals an unexpectedly steep rise of the slope. Since such a strong dependence of the current on the illumination intensity is difficult to explain on the basis of the existing theories, Farkas and Korvath<sup>[59]</sup> undertook a more detailed investigation. They found that the observed features were partly due to the structure of a train of pulses investigated in Ref. 55. In those cases when the  $Q$  factor was switched by a bleachable filter with a low initial absorption, the generated pulses exhibited a regular structure which was disturbed only at the end of a pulse. When the initial absorption of the dye in the filter was high, the pulses were of about 50 psec duration even at the beginning of a train, there was a substructure with a period of the order of 10<sup>-13</sup> sec, and the spectral distribution was irregular. It was concluded in Ref. 59 that in the case of ultrashort laser pulses with a reproducible structure the theoretical predictions<sup>[23, 24]</sup> were confirmed qualitatively at moderate and high illumination intensities. In the case of longer pulses with an irregular and poorly reproducible structure, the observed rise of the order of nonlinearity could be due to a new type of thermionic emission discussed in Refs. 21 and 22. A detailed investigation of this point was made<sup>[60, 61]</sup> using giant pulses whose duration was a few tens of picoseconds. A single picosecond pulse was separated from a train by a Pockels cell and passed through three amplifying stages. A master oscillator, which was a YAG:Nd laser, was operated in the mode-locked regime and emitted a single transverse mode. The pulse shape was recorded with an image-converter camera and was found to be Gaussian of 30 psec half-width. The other details of the apparatus were identical with those used in Ref.

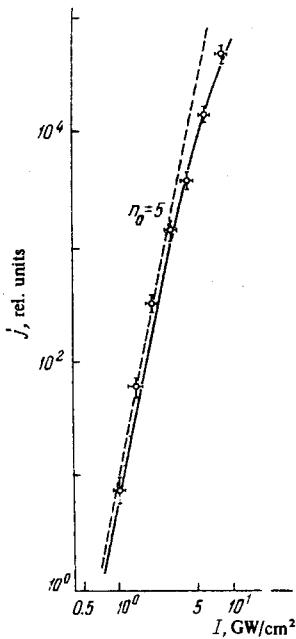


FIG. 25. Reduction in the degree of nonlinearity (order of the photoelectric effect) with increasing illumination intensity.

59. The experiments were carried out on a gold cathode. A beam fell tangentially on the cathode surface and the vector  $\vec{\varepsilon}$  was directed at right-angles to the surface.

The results are plotted in Fig. 25 on a double logarithmic scale as the dependence of the emission current on the illumination intensity (in relative units). Each point in Fig. 25 is the average of 20 measurements. Right up to intensities of a few gigawatts per square centimeter, the lux-ampere characteristic remains a straight line with a slope of 5, i. e., the pure five-photon effect takes place. Deviations from this dependence begin when the field intensity is  $\varepsilon^* \sim 10^{6.3}$  V/cm, which is in agreement with the earlier results.<sup>[58, 59]</sup> It should be noted that the theoretical calculations<sup>[24]</sup> gives a much higher value of the critical field:  $\varepsilon^* \sim 10^{7.3}$  V/cm. It is pointed out in Refs. 23, 54, and 62 that in calculations of the critical field one has to allow for the Cou-

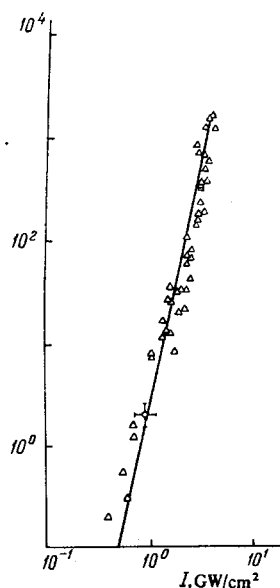


FIG. 26. Photoelectric current  $j$  (A/cm<sup>2</sup>) from the surface of tungsten illuminated with picosecond pulses.

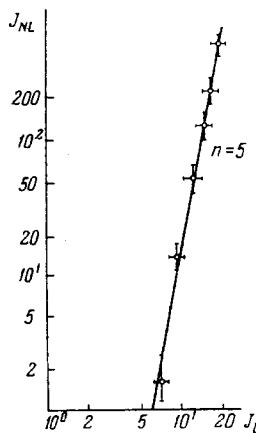


FIG. 27. Photoelectric emission under the action of a single picosecond pulse free of substructure (Au, neodymium laser).

lomb interaction of the emitted electrons with the metal. However, the estimates obtained in Refs. 23 and 54 allowing for this effect give a very low value for the critical field,  $\varepsilon^* \sim 10^5$  V/cm, which again does not agree with the experimental results. We shall return to this difficulty in Sec. 5, where we shall discuss the theory of the nonlinear photoelectric effect.

In principle, the discrepancy between the theoretical and experimental values of the critical field may be due to inaccuracy of the experimental determinations of this field. However, it is unlikely that such an inaccuracy may result in a tenfold reduction in the field intensity.<sup>2)</sup>

Similar measurements on a tungsten cathode, carried out with the same apparatus as in Refs. 60 and 61, were described in Ref. 62. Many-photon electron emission with  $n = 4$  (Fig. 26) was observed for values of  $\varepsilon_1$  not exceeding  $10^{6.2}$  V/cm (the intensity was calculated at the maximum of a laser pulse). Thus, the results reported in Refs. 60–62 indicated that smooth single picosecond pulses caused photoelectric emission with a degree of nonlinearity  $n = n_0 = (1 + (A/\hbar\omega))$  and it was not possible to observe values of  $n$  exceeding  $n_0$ . It was shown earlier in Ref. 59 that the emission with  $n > n_0$  occurred in the falling part of a train of picosecond pulses in approximately the same range of intensities. Such anomalous emission with  $n > n_0$  could be due to the properties not of the pulse train but of the structure of the individual pulses and this was tested in Ref. 63 by investigating the emission under the action of single picosecond pulses of two types: a) smooth Gaussian pulses of  $\sim 6$  psec duration, separated from the part of the train of growing intensity, and b) pulses with a definite substructure of  $\sim 50$  psec duration obtained using a bleachable filter with a high initial absorption. It was found that type a) pulses caused photoelectric emission with  $n = n_0 = 5$  (Au cathode, neodymium laser). The lux-ampere characteristic obtained in this case is shown in Fig. 27.

In the case of type b) pulses (Fig. 28) the values were  $n > n_0$ . The emission current also depended strongly on the polarization of the incident radiation. It was impossible to measure accurately the intensities of type b)

<sup>2)</sup> These values of  $\varepsilon^*$  were calculated from the radiation intensities averaged with respect to time and over the focusing spot.

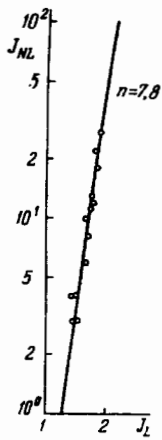


FIG. 28. Photoelectric emission under the action of a single picosecond pulse with a strong substructure (Au, neodymium laser).

pulses but an estimate based on the measured parameters gave a value of the order of a few gigawatts per square centimeter.

The appearance of emission with  $n > n_0$ , together with strong polarization dependences in the case of type b) pulses indicated that the observed current was a superposition of photocurrents of different orders of nonlinearity, which were excited simultaneously. This type of emission was predicted in Ref. 64, where it was shown that values of  $n = d(\ln j)/d(\ln I)$  for the total current could exceed  $n_0$ .

### B. Dependence of emission current on polarization of radiation

Since the surface and bulk photoelectric effects and thermionic emission can have similar lux-ampere characteristics in a narrow range of illumination intensities, the knowledge of these characteristics is insufficient for the identification of the emission mechanism. In view of this, measurements were made<sup>(60)</sup> of the polarization dependence of the emission current. The measurement method was basically similar to that described above (Sec. 2). The direction of polarization of light incident on the cathode was varied by rotation of a Glan-Thompson prism placed in the laser beam. The measurements were carried out in the range of intensities where the relationship  $j \propto I^n$  was obeyed. The parallel  $\mathcal{E}_{\parallel}$  and perpendicular  $\mathcal{E}_{\perp}$  components of the electric field depended on the orientation of the original (in the absence of the prism) polarization of the laser beam relative to the cathode surface. We shall consider two cases.

In the first case (Fig. 29), the direction of polarization of the incident beam is described by the angle  $\varphi$  between the oscillation plane of the electric vector and the normal to the cathode surface. Then, the field components are

$$\begin{aligned} \mathcal{E}_{\perp}(\varphi) &= \mathcal{E}_0 \cos^2 \varphi, \\ \mathcal{E}_{\parallel}(\varphi) &= \mathcal{E}_0 \cos \varphi \sin \varphi. \end{aligned}$$

It is clear from Fig. 29 that the measured photocurrent depends only on the component of the field  $\mathcal{E}_{\perp}$  and is described by

$$j = |\mathcal{E}_{\perp}(\varphi)|^{2n} = \mathcal{E}_0^{2n} \cos^{2n} \varphi,$$

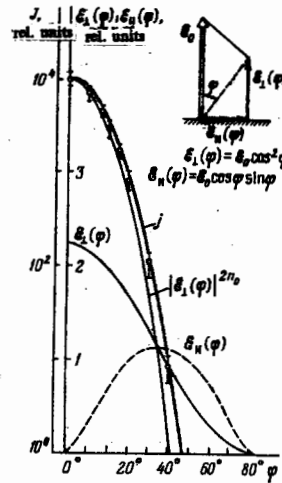


FIG. 29. Polarization dependence of the photoelectric current. The experimental configuration is shown in the top right-hand corner.

which corresponds to the fifth-order surface photoelectric effect. The influence of the field component parallel to the surface cannot be observed even for the maximum value of this component  $\mathcal{E}_{\parallel} = \mathcal{E}_0/2$ .

In the second case (Fig. 30), the field components are governed by the angle  $\alpha$  between the oscillation plane of the electric vector and the cathode surface. If this surface makes an angle of  $45^\circ$  with the original direction of polarization of the electric vector, the dependence of the field components on  $\alpha$  is given by

$$\begin{aligned} \mathcal{E}_{\perp}(\alpha) &= \mathcal{E}_0 \cos\left(\frac{\pi}{5} - \alpha\right) \sin \alpha, \\ \mathcal{E}_{\parallel}(\alpha) &= \mathcal{E}_0 \cos\left(\frac{\pi}{4} - \alpha\right) \cos \alpha. \end{aligned}$$

The maximum values of the field components are  $\mathcal{E}_{\perp \max} = \mathcal{E}_{\parallel \max} = \mathcal{E}_0/\sqrt{2}$ .

The experimentally determined dependence of the emission current on the angle  $\alpha$  agrees with the expected law

$$j \propto |\mathcal{E}_{\perp}(\alpha)|^{2n} = \mathcal{E}_0^{2n} \left[ \cos\left(\frac{\pi}{4} - \alpha\right) \sin \alpha \right]^{2n}$$

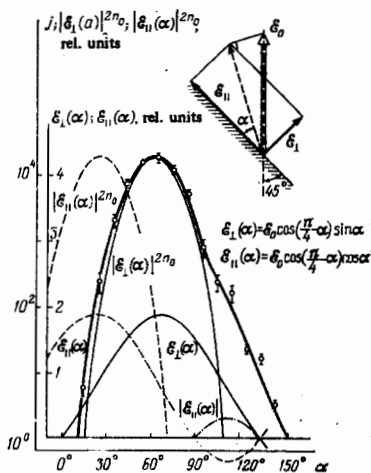


FIG. 30. Polarization dependence of the photoelectric current for a modified configuration (shown in the top right-hand corner).

throughout almost the whole range of  $\alpha$ . It is interesting to note a slight discrepancy for angles  $\alpha \gtrsim 90^\circ$ . It is important to note that the current is governed only by the normal component of the field even in the region of maximum  $\mathcal{E}_\parallel$  and deviations from this dependence begin at  $\alpha \approx 90^\circ$  where the component  $\mathcal{E}_\parallel$  changes its sign. This unexpected observation requires further study.

It is interesting that the strong polarization dependence is observed not only for smooth pulses but also for single pulses with a substructure which give rise to a lux-ampere characteristic of slope  $n > n_0$ .<sup>[63]</sup>

Summarizing the above results, we may conclude that in the investigated case (Au cathode, neodymium laser) the electron emission is entirely due to the surface photoelectric effect. The change in the lux-ampere characteristic with increasing field intensity is in qualitative agreement with the theoretical predictions. The anomalous change in this characteristic observed in some experiments and the slopes with  $n > n_0$  are due to an irregular structure of the laser pulses.

## 5. THEORY OF NONLINEAR PHOTOELECTRIC EFFECT

The one-photon case has been analyzed most thoroughly in the theory of the photoelectric effect. Relatively little work has been done on the many-photon emission of electrons and almost all this work has been concerned with the surface photoelectric effect.

The general approach to the problem makes it possible to divide the theoretical papers on the photoelectric effect into two natural groups. The first represents calculations of the photoelectric emission based on phenomenological models of the interaction of light with electrons in a metal. The simplest of these model theories, developed in Ref. 65, is one of the first applications of quantum mechanics to solid-state physics. The approach proposed in Ref. 65 has been found to be very fruitful and for a long time the theory of the photoelectric effect has been evolving by improvement of phenomenological models. The influence of the form of the potential barrier at the metal-vacuum interface, as well as the influence of temperature, nonideal nature of the surface, and periodic lattice field on the emission current have been investigated in turn. In spite of the patent inconsistency of the phenomenological approach, pointed out many times by its critics, and the extreme simplicity of the models employed, the results of the calculations have usually been found to be in very good agreement with the experimental data. The phenomenological approach has not lost its importance in the theory of the photoelectric effect even now. It is sufficient to mention that a considerable number of the results obtained in the theory of the bulk and nonlinear surface photoelectric effects is based on a model representation and is in reasonable agreement with the experimental results.

The second group comprises papers in which a consistent quantum-mechanical formulation of the problem of photoelectric emission is employed. The most important result of these investigations is the understand-

ing of the reasons for the success and determination of the limits of validity of the phenomenological theories of the effect. A very convenient (from the point of view of calculations) approach to photoelectric emission is based on the threshold approximation in the scattering problem.<sup>[23]</sup> A different but generally equivalent formalism is used in Refs. 66 and 67. It is important to note that the approach developed in Refs. 23, 66, and 67 makes it possible to allow in a natural manner for the many-electron effects.<sup>[35, 68]</sup> The main computation method in the papers belonging to the second group is the perturbation theory, which is very convenient in one-photon emission calculations. In the many-photon case the main interest lies in strong optical fields in which the condition of validity of the perturbation theory may not be obeyed. Some of the results are obtained for this case in Ref. 23 by allowance, within the scattering problem framework, for the interaction in the final state.

In this section we shall describe the main methods for the calculation of photoelectric emission and the results obtained by these methods. We shall pay special attention to the case of strong optical fields and to some effects which are characteristic of the linear method of photoemission excitation.

### A. Transient perturbation theory. Phenomenological approach

We shall begin with model calculations of the photoelectric emission current in fields which are weak compared with the intra-atomic fields. Calculations of the kind have been carried out by many authors (see Ref. 19) for the one-photon effect; the two-photon emission is considered in Refs. 13 and 69 and the three-photon case in Ref. 33. The model nature of the calculations results from the fact that an analysis is made not of the interaction of light with a metal but of the absorption of light by an electron in some one-dimensional potential field. In most cases, the Sommerfeld model is used in which the potential is in the form of a step:  $V(x) = V_0 \theta(x)$ . The external field is assumed to be weak and is regarded as a perturbation.

The motion of an electron in the field of an optical wave and of this potential is described by the Schrödinger equation

$$i\hbar \frac{\partial \psi}{\partial t} = \mathcal{H} \psi \quad (6)$$

with the Hamiltonian

$$\mathcal{H} = -\frac{\hbar^2}{2m} \Delta + V(x) + \frac{ie\hbar}{mc} \mathbf{A} \nabla + \frac{e^2}{2mc^2} \mathbf{A}^2,$$

where  $\mathbf{A}(\mathbf{r}, t)$  is the vector potential of the optical wave; the rest of the notation is standard. The current, considered as a function of the electron momentum, is calculated in the usual way from the solution of Eq. (6):

$$\mathbf{j}(\mathbf{p}) = \frac{ie\hbar}{2m} (\psi \nabla \psi^* - \psi^* \nabla \psi) - \frac{e^2}{mc} \mathbf{A} \psi^* \psi.$$

The current density is found by averaging over the Fermi distribution  $W(\mathbf{p})$ :



$$j = \int dp W(p) j(p). \quad (7)$$

In a weak field the solution of the Schrödinger equation (6) can be found in the form of a series in powers of the vector potential. Substituting in Eq. (6) the potentials  $V(x) = V_0 \theta(x)$  and  $A = a \cos \omega t$ , we can write the wave function in the form

$$\psi = \sum_{n=0}^{\infty} \psi_n \exp \left[ -i \left( kx + \frac{E}{\hbar} \right) \right], \quad (8)$$

where  $E = p^2/2m$  is the electron energy in the absence of the field and  $\psi_n \propto |a|^n \propto |E_0 c/\omega|^n$ .

We shall follow the treatment of Ref. 70, where the perturbation theory calculations are made of the photoelectric emission of an arbitrary order. The formulas of Refs. 13, 19, 33, and 69 follow as special cases from the results of Ref. 70. We shall assume that the incident electromagnetic field penetrates the metal. This assumption is more natural in the case of the surface photoelectric effect than the assumption that there is a field discontinuity at the surface. The discontinuities of the field and the effective electron mass on the surface can make an additional contribution to the photoexcitation and allowance for them should generally increase somewhat the emission current. If necessary, these effects can be included in an obvious manner in the calculations reported below.

Substituting Eq. (8) into Eq. (6) and adopting (for convenience) the atomic units, we obtain a chain of equations for the functions  $\psi_n$

$$\left( -\frac{1}{2} \Delta + V(x) - E - kx \right) \psi_n + \frac{i\mathcal{E}_0}{2\omega} \nabla \psi_{n-1} + \frac{\mathcal{E}_0^2}{8\omega^2} \psi_{n-2} = 0. \quad (9)$$

Since the coefficients in these equations are piecewise-constant, the solution of Eq. (9) can be written in the form of a combination of exponential functions and the coefficients in front of these functions are found from the conditions of matching of  $\psi_n$  and their derivatives at  $x=0$ . Omitting the details of the calculations, we shall now give the final expression for the current density (in terms of dimensional variables):

$$j_n = \int_{M_n}^{\infty} dp_x f_n(p_x) \ln \left\{ 1 + \exp \left[ \frac{E_F - (p_x^2/2m)}{kT} \right] \right\}, \quad (10)$$

$$f_n(p_x) = \frac{\sqrt{2}}{\pi^2} \frac{ekT}{mch^3} p_x^2 V \sqrt{p_x^2 + 2m(n\hbar\omega - V_0)}$$

$$\times \left| D_n \left[ i \sqrt{n + \frac{p_x^2}{2m\hbar\omega}} \right] \right|^2 \left( \frac{e^2 \mathcal{E}_0^2}{2m\hbar\omega^3} \right)^n,$$

$$M_n = \begin{cases} 0, & V_0 < n\hbar\omega, \\ \sqrt{2m(V_0 - n\hbar\omega)}, & V_0 > n\hbar\omega. \end{cases}$$

where  $D_n(x)$  is some function for which a recurrence formula is given in Ref. 70. For  $n=0$  the formula (10) gives the thermionic emission current. For  $n=1, 2$ , or 3 we obtain the results known from Refs. 13, 19, 33, and 69.

A calculation of the quadrature in Eq. (10) for a known dependence of the cathode temperature on the laser illumination intensity makes it possible to determine the lux-ampere characteristic of the nonlinear photoelectric field. In many cases the effects associated with heating

are ignored and the integrals of the (10) type are calculated at  $T=0$ . If such a calculation is made in the present case, it is found that the dependence of the photocurrent on the component of the electric field of the wave normal to the cathode is described by a power law. By way of example, the dashed line in Fig. 31 is used for the lux-ampere characteristic of Ag and neodymium glass laser radiation, calculated without allowance for the photocathode heating. This line represents the dependence  $j \propto I^5$ . The continuous curve in the same figure shows the real lux-ampere characteristic obtained allowing for the photocathode heating (a calculation of the latter characteristic is described below). In addition to the clear difference between the curves at high intensities, one should note that the emission current represented by the continuous curve depends not only on the component of the electric field normal to the metal surface but also on the tangential components. The total current, representing a sum of the partial currents with different degrees of nonlinearity, exhibits a complex polarization dependence.

It is clear from Eq. (10) that the expansion in Eq. (8) is in terms of the powers of the parameter  $\Delta/\hbar\omega \approx e^2 \mathcal{E}_0^2 / m\hbar\omega^3$ . Therefore, the perturbation theory is valid only if the energy of classical oscillations of an electron in the field of an optical wave is low compared with the work function. In estimating the range of validity of the solution obtained by the perturbation theory and the nature of deviations from this solution we have to adopt the approach which does not require the assumption that the wave field is weak. This approach was first proposed by Keldysh<sup>[50]</sup> and applied to photoelectric emission in Refs. 15 and 24. We shall now consider some results obtained in these papers.

## B. Photoelectric emission at high radiation intensities. Limits of validity of perturbation theory

The transition of an electron to its final state because of its motion in the field of a strong optical wave is considered in Refs. 15, 24, and 50. This allows exactly for the effect of a strong field of a free electron. It is shown in Ref. 62 that the main results of Ref. 50 can be obtained more simply by the quasiclassical method. However, we shall follow the method of Ref. 50, because, for a simpler model of a metal, it makes it possible to obtain essentially the exact solution of the problem of nonlinear photoelectric emission.<sup>[24]</sup> Naturally, this

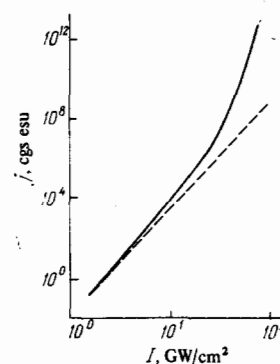


FIG. 31. Photoelectric emission from silver calculated on the basis of the perturbation theory: the continuous curve is obtained allowing for the cathode heating and the dashed curve—ignoring this heating.

gives rise to certain computational difficulties which require the application of numerical methods in the determination of the lux-ampere characteristics.<sup>[22]</sup>

The Sommerfeld model of a metal is used in Ref. 24: in this model electrons are regarded as particles with an effective mass and they are assumed to obey the Fermi statistics and to move in the field of a static potential. At the boundary of the metal the potential has a discontinuity  $V_0$ . The motion of an electron is described by a time-dependent Schrödinger equation (the atomic system of units is used):

$$i \frac{\partial \psi}{\partial t} = \mathcal{H} \psi.$$

The Hamiltonian is  $\mathcal{H} = \mathcal{H}_0 + \mathcal{H}_{\text{int}}$ , where  $\mathcal{H}_0 = -(1/2) \Delta - V_0 \theta(-x)$  and

$$\mathcal{H}_{\text{int}} = \theta(x) \left( -\frac{E \sin \omega t}{\omega} \mathcal{E}_0 \nabla + \frac{\mathcal{E}_0^2}{2\omega^2} \sin^2 \omega t \right). \quad (11)$$

The form of  $\mathcal{H}_{\text{int}}$  corresponds to the model in which the field does not penetrate into the metal (it is this case that is considered in Ref. 24). The solution can be generalized in the case of arbitrary field discontinuity at the metal surface. One has to add to  $\mathcal{H}_{\text{int}}$  a term analogous to Eq. (11) with  $\tilde{\mathcal{E}}_0$  instead of  $\mathcal{E}_0$  and with  $\theta(-x)$  instead of  $\theta(x)$ , and the expressions for the wave functions have to be modified by suitable factors.

The solutions of the Schrödinger equation in the regions  $x < 0$  and  $x > 0$  are obtained in Ref. 24 and these solutions are matched at the metal-vacuum interface. The matching condition represents an infinite system of transcendental equations, whose general solution is quite difficult to obtain. However, an analysis shows that if the field intensity satisfies the conditions

$$\left| \frac{\mathcal{E}_0^2}{4\omega^2} \right| \ll 1, \quad \left| \frac{\mathcal{E}_0^4}{256\omega^6} \right| \ll 1, \quad (12)$$

the system of equations can be simplified and its approximate solution can be found. Details of fairly cumbersome calculations are given in Ref. 24. We note that even after simplifications the calculation of the integral (7) is fairly difficult and it is carried out in Ref. 24 using the theorem on averages. The final result for zero cathode temperature is

$$j_m(\mathcal{E}_0, \omega) = (m!)^2 \left( \frac{\mathcal{E}_0^2}{2\omega^2} \right)^m \frac{2E_0^2}{3\pi^2 (m\omega)^m (2\omega)^{1/2}} \times \left[ 1 - \frac{1}{2} \theta(\Gamma - m\omega) \left( \frac{\Gamma - m\omega}{E_F} \right) \left( 5 - 3 \frac{\Gamma - m\omega}{E_F} \right) \right] \bar{C}, \quad (13)$$

where

$$\Gamma = V_0 + \frac{\mathcal{E}_0^2}{4\omega^2}, \quad m = \left\langle \frac{1 + (\mathcal{E}_0^2/4\omega^2)}{\omega} + 1 \right\rangle, \quad \bar{C} \approx 1.$$

The general appearance of Eq. (13) resembles the formulas obtained using the perturbation theory. However, there is an important difference: Eq. (13) includes the depth of the potential well  $\tilde{V}$ , which is measured not from the vacuum level but from the average energy of electron oscillations in the wave field  $\mathcal{E}_0^2/4\omega^2$ . The dependence of the emission current on the illumination intensity is a power law. However, the power exponent depends weakly on the illumination intensity.

The conditions (12) used in the derivation of Eq. (13) are satisfied if

$$\gamma = \frac{\omega}{\mathcal{E}_0} \sqrt{2V_0} \gg \frac{V_0}{\omega} \approx n.$$

The parameter  $\gamma$  on the left-hand side of the inequality has a simple meaning<sup>[15,50]</sup>: it is equal to the ratio of the frequency of light to the tunneling frequency and the latter is equal to the reciprocal of the time taken by an electron to tunnel across the potential barrier. The values  $\gamma \ll 1$  correspond to that range of light frequencies and field intensities in which the tunnel transition occurs in a time much shorter than the field period. In this limit the current is described by the well-known formulas for the emission in a static electric field.<sup>[71]</sup> According to Refs. 15 and 50, the perturbation theory should correspond to the opposite limiting case  $\gamma \gg 1$ . An analysis<sup>[24]</sup> shows, however, that in the case of photoelectric emission of higher orders  $n$  the condition of validity of the perturbation theory is much more stringent:  $\gamma \gg n$ . It is demonstrated in Ref. 24 that in the intermediate range  $1 < \gamma < n$  the slope of the lux-ampere characteristic  $d(\ln j)/d(\ln I)$  becomes less than at low intensities, where the perturbation theory is valid. This result is in qualitative agreement with the experimental data; however, the measured field intensity at which deviations from the perturbation theory are observed differs by about an order of magnitude from the theoretical estimate. A probable reason for this discrepancy is the fact that the Coulomb interaction of the emitted electrons with the surface of the metal is not allowed for in Ref. 24. The Coulomb corrections are included in a different solution method in Ref. 23. The same effect in an analogous problem of many-photon ionization of atoms is considered in Refs. 72 and 73 (for the review see Ref. 62). The methods used in these investigations do not provide rigorous quantitative results in the range of field intensities of practical interest. However, it is clear that allowance for the Coulomb interaction increases the size of the spatial region in which the potential gradient differs from zero and the photoionization probability increases. This reduces the critical field intensity at which the degree of nonlinearity of the process changes. These conclusions are in qualitative agreement with the experimental results of studies of many-photon ionization of atoms and of the nonlinear photoelectric emission of electrons from the surfaces of metals under the action of laser radiation. However, the problem has not yet been solved quantitatively.

### C. Influence of cathode heating on photocurrent characteristics

The thermal effects are allowed for automatically if averaging in Eq. (7) is made using the cathode temperature, which depends on the illumination conditions. This temperature can be found by solving the problem of heat conduction in a metal heated by a laser pulse. This problem is discussed in detail in Refs. 8 and 30. We shall consider the most interesting case of the interaction of picosecond laser pulses with a metal.

The absorption of light in a metal results directly in

an increase in the electron energy; the lattice heating is due to the relatively slow relaxation process whose dynamics can be described conveniently in terms of the Cerenkov emission of phonons by nonequilibrium electrons.<sup>[74]</sup> The characteristic time representing the lattice heating by exchange of energy with electrons is of the order of  $10^{-10}$  sec. In the case of shorter laser pulses the lattice heating is negligible during a pulse. Bearing in mind that at temperatures much lower than the Fermi energy the specific heat of the electron subsystem is small, we can readily see that electrons absorb energy and are heated in a very short time to some quasisteady temperature governed by the balance between the power received from an optical wave and the power dissipated in the form of Cerenkov emission of phonons and flow of heat into the metal. Thus, the temperature of the electron subsystem obeys the equation

$$\frac{\partial}{\partial x} \left( \chi_e \frac{\partial T_e}{\partial x} \right) - \alpha T_e - (1-R) \frac{\partial I(x, t)}{\partial x} = 0 \quad (14)$$

where  $\alpha$  is the coefficient representing heat exchange between the electrons and the lattice; according to Ref. 74, this coefficient is  $10^{17}$  erg · cm<sup>-3</sup> · sec<sup>-1</sup> · deg<sup>-1</sup>. It follows from Eq. (14) that the temperature of the surface is

$$T_e(0, t) \approx \frac{(1-R) I(0, t)}{\sqrt{\alpha \chi_e}} \quad (15)$$

The important point is that, because of the small specific heat of electrons, their temperature follows instantaneously the laser radiation intensity and, therefore, thermionic emission suffers practically no delay relative to the laser pulse. In fact, the electron specific heat is finite and some delay, of the order of  $c_e / \alpha \sim (c_e / \alpha) k T_e / E_F \sim 10^{-12}$  sec, does take place. A more rigorous calculation of the electron temperature and the thermionic emission can be found in Ref. 21. It follows from this calculation that in the case of laser pulses whose duration range is from a few picoseconds to a few tens of picoseconds the electron temperature can be regarded quite accurately as a function of the instantaneous laser radiation intensity, so that we can speak of the usual lux-ampere characteristic when the photocathode is heated significantly. (In general, when the temperature is delayed relative to the laser pulse, we can speak only of the dependence of the total emitted charge on the laser pulse parameters.)

We shall now consider how the cathode heating affects the lux-ampere characteristic. Let us assume that at

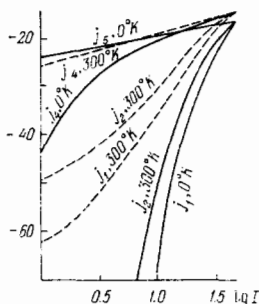


FIG. 32. Dependences of the various components of the emission current on the illumination intensity (Au, neodymium laser).

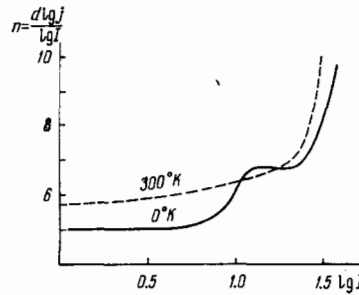


FIG. 33. Dependences of the nonlinearity order on the illumination intensity (Au, neodymium laser).

zero cathode temperature the minimum number of photons necessary to knock out an electron is  $n_0$ . Heating of the cathode produces electrons with energies above the Fermi level, so that emission can now take place as a result of absorption of fewer than  $n_0$  photons. We can easily see that the order of magnitude of the ratio of the  $n$ -photon and  $(n-1)$ -photon currents is

$$\frac{j_n}{j_{n-1}} = c_n \frac{\Delta}{\hbar \omega} \exp \left( \frac{\hbar \omega}{kT} \right) = c_n \xi(I),$$

where

$$\xi(I) = \frac{I}{I_2} \exp \left( \frac{I_1}{T_0 + T} \right),$$

$$I_0 = \frac{T_0 \sqrt{\alpha \chi_e}}{1-R} \sim \frac{10^5 T_0}{1-R}, \quad I_1 = \frac{\hbar \omega I_0}{k T_0} \sim \frac{10^{-8} \omega}{1-R}, \quad I_2 = \frac{m c \hbar \omega^3}{2 \pi e^2} \sim 2 \cdot 10^{-3} \omega^3$$

and  $T_0$  denotes the initial cathode temperature. The above formulas are derived from Eq. (15). The total current is

$$j = j_{n_0} P(\xi),$$

where  $P(\xi)$  is a polynomial of degree  $n_0$ . A calculation of the nonlinearity coefficient of the total current,

$$n = \frac{d \ln j}{d \ln I} = n_0 + \delta(I).$$

readily shows that at low intensities  $I < I_0^2 / I_1$  the correction  $\delta(I)$  due to thermal effects is negative, which is in agreement with the experimental results.<sup>[11]</sup> At  $I \sim I_0^2 / I_1$  the correction  $\delta(I)$  changes its sign and remains positive right up to intensities of the order of  $I_1$ . Thus, the observed slope of the lux-ampere characteristic depends in a fairly complex manner on the illumination intensity.

These estimates demonstrate that a rigorous allowance for thermal effects in many-photon emission is necessary. Calculations making this allowance are reported in Ref. 22. The partial currents considered as a function of the electron quasimomentum and representing the absorption of  $n_0, n_0 - 1$ , etc. photons are calculated by numerical methods using the Silin model.<sup>[24]</sup> Next, the results are averaged over a Fermi distribution with a temperature which is a function of the laser intensity.<sup>[21]</sup> The results of a calculation for Au and neodymium laser radiation ( $n_0 = 5$ ) are presented in Figs. 32 and 33. Figure 32 gives the dependences of the averaged partial currents from  $n = 1$  to 5 on the illumination intensity. The curves are calculated for two values of the initial temperature and the cathode reflec-

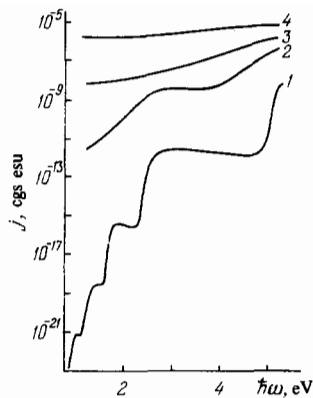


FIG. 34. Dependences of the photocurrent on the photon energy for different illumination intensities ( $\text{W}/\text{cm}^2$ ): 1)  $10^9$ ; 2)  $4 \times 10^{10}$ ; 3)  $7 \times 10^{10}$ ; 4)  $10^{11}$ . Silver cathode; calculations based on the perturbation theory.

tion coefficient  $R = 0.99$ . The dependence of the nonlinearity coefficient of the total current on the laser radiation intensity is plotted in Fig. 33. It follows from the calculations of Ref. 22 that in the range of intensities considered the correction  $\delta(I)$  is positive. When the intensities are of the order of  $15 \text{ GW}/\text{cm}^2$ , the main five-photon current has to be supplemented by the four-photon contribution, which rapidly rises with the intensity. At  $I \sim 40 \text{ GW}/\text{cm}^2$  the contributions of all transitions with  $n \leq 4$  become of the same order of magnitude. The contribution of the current  $j_6$  is then negligibly small.

A similar calculation of the lux-ampere characteristic of silver for neodymium laser radiation is given in Ref. 70. The current densities are calculated as a function of the electron quasimomentum using the perturbation theory developed in Ref. 70. Next, the results are averaged over an energy distribution of electrons with a temperature calculated in Ref. 21. The results are represented by the continuous curve in Fig. 31. For comparison, this figure includes the characteristic of the five-photon emission (dashed line). The dependence of the photocurrent on the laser radiation frequency (Fig. 34) is also calculated in Ref. 70. This calculation is carried out for a silver photocathode. We can see that the dependence of the emission current on the laser radiation frequency is not monotonic. However, at high intensities the cathode heating mixes currents of different orders and this smooths out the frequency dependence of the total current.

It is pointed out in Sec. 4 that a qualitative confirmation of the above calculations is provided by the experiments reported in Ref. 63, where it is found that the nonlinearity coefficient is higher for pulses with an irregular structure than for smooth pulses of the same intensity. Since in the case of irregular pulses the instantaneous values of the intensity may be considerably higher than the average in a pulse, we can naturally expect stronger cathode heating than in the case of smooth pulses and this may be the reason for the observed increase in the nonlinearity.

However, this interpretation is not the only one possible. A different explanation of the results of Ref. 63 is given in Ref. 75. According to Ref. 75, the emission mechanism is of the two-stage type: initially the absorption of light excites surface plasmons in a metal;

then, plasmons interact with electrons producing an emission current. Since the plasmon energy is higher than the work function, the nonlinearity coefficient should be higher than  $n_0$ . Clearly, additional experiments are needed to determine more reliably the mechanism of emission characterized by anomalously high nonlinearity exponents.

#### D. Analysis of surface photoelectric effect based on theory of threshold phenomena

An important task of the theory of nonlinear photoelectric emission is to justify and find the limits of validity of the phenomenological approach, which has yielded a large number of important results. The crucial question is to what degree the results of the phenomenological treatment are related to the actual features of a specific model. A fairly full answer to this question can be found in a series of papers by Brodskii and Gurevich which are presented in a monograph.<sup>[23]</sup> In the case of the linear photoelectric effect the same question is tackled by different methods in Refs. 66 and 67. Since exhaustive information on the current status of this problem can be found in Ref. 23, we shall not consider details and give only the formulation of the problem and the main results.

Photoelectric emission of electrons is considered in Ref. 23 as the inelastic scattering of photons by a metal. A general analysis of such scattering can be carried out without invoking a specific model of the scatterer but using the threshold approximation. The main assumption underlying the threshold approximation is that the final electron energy is small compared with the binding energy of an electron in a metal. The emission current can be calculated by finding the wave functions of the final state. After isolation of the time factor, the coordinate parts of these functions satisfy—at large distances  $x > x_0$  from the surface—the Schrödinger equation

$$\left[ \frac{d^2}{dx^2} + p^2 - 2V(x) \right] \psi = 0.$$

In the  $n$ -photon emission case, we have

$$p^2 = 2E_j - p_0^2, \quad E_j = E_i + n\omega.$$

The potential  $V(x)$  describes the Coulomb interaction of the emitted electron with the surface,  $V(x) = (2\epsilon x)^{-1}$ , and  $\epsilon$  is the permittivity. This interaction can be ignored for emission in an electrolyte. The known asymptotic solutions of the above equation can be used to calculate the current at large distances from the surface:

$$j(p) = p |\Lambda|^2 |C_0|^2, \quad C_0^2 = \frac{\mu}{\exp \mu - 1}, \quad \mu = -(4\epsilon p)^{-1}.$$

The factor  $|\Lambda|^2$ , which occurs in the expression for  $j(p)$ , is governed by the interaction of an electron with a light wave in a surface layer, where the potential gradient is high, and it cannot be found in its general form. If we adopt the model of free electrons in a potential well of depth  $V_0$ , we find that a calculation<sup>[14, 61]</sup> gives  $|\Lambda^{(1)}|^2 = 2E_F \xi_1^2 / \omega^4$  for the one-photon surface effect. When a large number of photons is absorbed, the

perturbation theory gives an order-of-magnitude estimate  $|\Lambda^{(n)}|^2 \sim |\Lambda^{(1)}|^2 (g_1^2/\omega^3)^{n-1}$ . Using this expression and averaging the current over the electron energy distribution, we obtain the following formula for the  $n$ -photon emission current (dimensionless variables):

$$j_n = \frac{m(kT)^2}{2\pi^2\hbar^3} |\Lambda^{(n)}|^2 \sqrt{\frac{E_e}{E_F}} \int_0^\infty dx [1 - \exp(-\sqrt{\frac{\sigma}{x}})]^{-1} \ln(1 + e^{\beta(\omega-x)}),$$

where

$$\sigma = \frac{E_e}{kT}, \quad \beta = \frac{\hbar(n\omega - \omega_0)}{E_e},$$

$$E_e = \frac{\pi^2 e^4}{8\epsilon^2 \hbar^2} \quad \text{and} \quad \omega_0 = \frac{A}{\hbar}.$$

In the limit of low temperatures we find that in the case of emission in vacuum,

$$n = \begin{cases} 0, & n\omega < \omega_0, \\ \frac{m}{4\pi^2\hbar^2} |\Lambda^{(n)}|^2 \sqrt{\frac{E_e}{E_F}} (n\omega - \omega_0)^2, & n\omega > \omega_0. \end{cases}$$

In the case of emission in a dielectric, the expression for the current depends on the parameter  $\beta$ . In the immediate vicinity of the threshold, when  $\beta \ll 1$ , we obtain the same result as for the emission in vacuum. However, if  $\epsilon$  is sufficiently high, we can have the case  $\beta \gg 1$ , when the image forces do not affect the electron motion. The result is then

$$j_n = \frac{2m}{15\pi^2\hbar^3/2} E_F^{-1/2} |\Lambda^{(n)}|^2 (n\omega - \omega_0)^{5/2} \quad (n\omega > \omega_0).$$

This formula was confirmed by investigations of photoelectric emission in electrolytes.

### E. Comments on the bulk nonlinear photoelectric effect

So far our discussion has been concerned mainly with the surface photoelectric effect in which the absorption of light is limited by the potential gradient in the surface layer. Another reason for the absorption of light in metals is the scattering of electrons by phonons and impurities in the bulk. This mechanism may be responsible for the bulk photoelectric effect. The considerable physical differences between the surface and bulk effects were pointed out by Tamm and Shubin.<sup>[76]</sup>

The nature of absorption is usually found experimentally from the polarization dependence of the photocurrent. Measurements of the nonlinear photoelectric emission (Secs. 2 and 4) show that for  $n=3$  and  $n=5$  the photoelectric emission is of surface type. On the other hand, the results in Ref. 34 suggest that the two-photon effect in sodium is of bulk nature. The experiments described in Refs. 42-45 suggest bulk nature of the two-photon emission in an electrolyte solution. A considerable bulk component is also characteristic of the one-photon emission (see Refs. 37 and 77). Clearly, one of the reasons for the absence of the bulk component in the photoelectric emission with high degrees of nonlinearity is that the thickness of the layer in the metal in which the field intensity is sufficient for the generation of a significant photocurrent is  $n$  times smaller in the case of the  $n$ -photon process than in the one-photon case.

In the linear case the experimental data on the bulk

photoelectric effect are in good agreement with the phenomenological theory of Spicer *et al.*,<sup>[37, 48, 49]</sup> which treats emission as a sequence of three processes: optical excitation of electrons in the bulk of a metal, motion of some of the excited electrons to the surface, and subsequent overcoming of the surface barrier. In the simplest case the scattering of electrons in the bulk and their reflection from the surface are allowed for by introducing an effective depth of electron emission. In some cases (see, for example, Refs. 78 and 79), the motion of an excited electron toward the surface is considered in greater detail using the random walk model.

An obvious shortcoming of the theory of Ref. 37 is the division of the emission event into three separate stages, of which only the first is treated as a quantum transition. The validity of this division is not self-evident and this is the basis of the criticism of the Spicer model in Ref. 80. Comments on the validity of the model of Ref. 37 can also be found in Ref. 81.

An attempt to use the three-stage model in developing the theory of the bulk two-photon effect is made in Refs. 34 and 36. However, the probability of two-photon absorption transitions in a metal is not calculated and, therefore, the relationships found there cannot be compared directly with the experimental data.

The matrix elements of the transition are calculated by Brodskii and Tsarevskii,<sup>[81]</sup> who consider the problem of photoelectric emission from an isolated center with a spherically symmetric potential and then generalize this result to the model of a metal in which the wave functions for the bulk of the metal are governed by spherically symmetric potentials of the ionic cores in each cell. We shall not consider the details of this calculation (the reader is referred to Ref. 81) but we shall give the most important results. It is pointed out above that the ratio of the partial currents corresponding to the absorption of  $n$  and  $n-1$  photons at  $T=0$  is of the order of magnitude of the perturbation theory parameter  $\Delta/\hbar\omega \sim e^2 g^2/m\hbar\omega^3$ . In the case of the bulk photoelectric effect the ratio  $j_2/j_1$  is estimated to be

$$\frac{j_2}{j_1} \approx \frac{\Delta}{\hbar\omega} \left[ (\hbar\omega)^{-1} \frac{m}{\hbar^2} \left( \frac{r^2 \partial V(r)}{\partial r} \right)^2 \right],$$

where  $V(r)$  is the potential of the ionic core and the bar denotes averaging over a unit cell. Usually the expression in brackets amounts to a few tens so that the relative probability of the two-photon bulk photoelectric effect is considerably higher than that of the surface effect. This result is in agreement with the experimental data on the emission in an electrolyte solution,<sup>[43]</sup> where a direct measurement was made of the ratio of the two- and one-photon currents. The dependence of the bulk photocurrent on the angles of incidence and polarization of light is governed by the energy band structure of the metal. In the case of a metal with an  $s$  band and polarization of light in the plane of incidence ( $p$  polarization), the angular dependence is

$$j_{1p} \sim (\omega - \omega_0)^{\nu} \left[ \sin^2 \zeta + O\left(\frac{\omega - \omega_0}{\omega_0}\right) \right],$$

$$j_{2p} \sim (2\omega - \omega_0)^{\nu} \left[ \sin^4 \zeta + O\left(\frac{2\omega - \omega_0}{\omega_0}\right) \right],$$

where  $\zeta$  is the angle of transmission of light in the metal related to the angle of incidence by the Fresnel formulas<sup>[19, 82]</sup>;  $\nu = 2$  for the emission in vacuum and  $\nu = 5/2$  for the emission in an electrolyte. In the case of light polarized at right-angles to the plane of incidence (*s* polarization) the one-photon emission current is independent of the angle. The above formulas apply to the threshold range of energies  $|n\omega - \omega_0| \ll \omega_0$ . It follows from these formulas that the bulk photocurrent should exhibit a polarization dependence as strong as the surface photocurrent.

We should also mention that, according to Ref. 81, for normal incidence of light the quadratic Fowler law for the emission in vacuum should change to the cubic form. The deviation from the Fowler law for the photoelectric emission from copper single crystals<sup>[83]</sup> may be regarded as confirmation of this theoretical prediction.

In the case of metals with a complex energy band structure, in which the initial state of an electron corresponds to a nonzero orbital momentum, the angular dependence of the two-photon current in the case of *p* polarization of the incident wave is given by

$$j_{2p} \sim (2\omega - \omega_0)^\nu (a \sin^4 \zeta + b \sin^2 \zeta \cos^2 \zeta + c \cos^4 \zeta),$$

where the constants *a*, *b*, and *c* may be of the same order of magnitude so that—in contrast to the surface photoelectric effect—the photocurrent resulting from the normal incidence of light may be comparable with that generated by light which is obliquely incident.

Thus, the existing theoretical models of the nonlinear photoelectric effect explain satisfactorily the experimental data. A very considerable progress has been made in the understanding of the photoelectric effect in strong optical fields. However, some fine details of this effect, particularly the dependence of the emission current on the frequency of light in a nonthreshold photomultiplier, as well as the relationship the angular and polarization dependences of this current to the energy band structure of the metal, require further theoretical and experimental studies. The current status of the theory and experiment makes it possible to give a quantitative description of the main features of the many-photon emission of electrons.

The authors are deeply grateful to S. D. Babenko, J. Bergou, A. M. Brodskii, N. B. Delone, N. A. Inogamov, I. I. Kantorovich, N. Kroć, and Z. G. Horváth for much valuable advice and their help at different stages.

<sup>1</sup>N. B. Delone, Usp. Fiz. Nauk 115, 361 (1975) [Sov. Phys. Usp. 18, 169 (1975)].

<sup>2</sup>J. Nuckolls, L. Wood, A. Thiessen, and G. Zimmerman, Nature (London) 239, 139 (1972).

<sup>3</sup>K. A. Brueckner and S. Jorna, Rev. Mod. Phys. 46, 325 (1974).

<sup>4</sup>A. M. Prokhorov, S. I. Anisimov, and P. P. Pashinin, Usp. Fiz. Nauk 119, 401 (1976) [Sov. Phys. Usp. 19, 547 (1976)].

<sup>5</sup>V. S. Letokhov and C. B. Moore, Kvantovaya Elektron. (Moscow) 3, 248, 485 (1976) [Sov. J. Quantum Electron. 6,

129, 259 (1976)].

<sup>6</sup>A. P. Kazantsev, Avtoreferat dokt. dissertatsii (Author's Abstract of Doctoral Thesis), Institute of Theoretical Physics, Academy of Sciences of the USSR, Moscow, 1976.

<sup>7</sup>I. B. Levinson, Fiz. Tekh. Poluprovodn. 7, 1673 (1973) [Sov. Phys. Semicond. 7, 1121 (1974)].

<sup>8</sup>S. I. Anisimov, Ya. A. Imas, G. S. Romanov, and Yu. V. Khodyko, Deĭstvie izlucheniya bol'shoi moshchnosti na metally (Effects of High-Power Radiation of Metals), Nauka, M., 1970.

<sup>9</sup>P. P. Barashev, Phys. Status Solidi A 9, 9 (1972).

<sup>10</sup>R. E. B. Makinson and M. J. Buckingham, Proc. Phys. Soc. London Sect. A 64, 135 (1951).

<sup>11</sup>M. C. Teich, J. M. Schroeder, and G. J. Wolga, Phys. Rev. Lett. 13, 611 (1964).

<sup>12</sup>G. Farkas, Z. S. Náray, and P. Varga, Phys. Lett. A 24, 134 (1967).

<sup>13</sup>R. L. Smith, Phys. Rev. 128, 2225 (1962).

<sup>14</sup>I. Adawi, Phys. Rev. 134, A 788 (1964).

<sup>15</sup>F. V. Bunkin and M. V. Fedorov, Zh. Eksp. Teor. Fiz. 48, 1341 (1965) [Sov. Phys. JETP 21, 896 (1965)].

<sup>16</sup>E. M. Logothetis and P. L. Hartman, Phys. Rev. 187, 460 (1969).

<sup>17</sup>A. D. Gladun and P. P. Barashev, Usp. Fiz. Nauk 98, 493 (1969) [Sov. Phys. Usp. 12, 490 (1970)].

<sup>18</sup>G. Farkas, in: Proc. First Conf. on Interaction of Electrons with Strong Electromagnetic Field, Balatonfüred, 1972, Invited Papers, publ. by Central Research Institute for Physics, Budapest (1973), p. 179.

<sup>19</sup>A. V. Sokolov, Opticheskie svoistva metallov, Fizmatgiz, M., 1961 (Optical Properties of Metals, American Elsevier, New York, 1967).

<sup>20</sup>F. V. Bunkin and A. M. Prokhorov, Zh. Eksp. Teor. Fiz. 52, 1610 (1967) [Sov. Phys. JETP 25, 1072 (1967)].

<sup>21</sup>S. I. Anisimov, B. L. Kapeliovich, and T. L. Perel'man, Zh. Eksp. Teor. Fiz. 66, 776 (1974) [Sov. Phys. JETP 39, 375 (1974)].

<sup>22</sup>S. I. Anisimov, N. A. Inogamov, and Yu. V. Petrov, Phys. Lett. A 55, 449 (1976).

<sup>23</sup>A. M. Brodskii and Yu. Ya. Gurevich, Teoriya fotoémissii iz metallov (Theory of Photoelectric Emission from Metals), Nauka, M., 1973.

<sup>24</sup>A. P. Silin, Fiz. Tverd. Tela (Leningrad) 12, 3553 (1970) [Sov. Phys. Solid State 12, 2886 (1971)].

<sup>25</sup>E. Panarella, Lett. Nuovo Cimento 3, 417 (1972).

<sup>26</sup>G. Farkas, Z. G. Horváth, I. Kertész, and G. Kiss, Lett. Nuovo Cimento 1, 314 (1971).

<sup>27</sup>D. Lichtman and J. F. Ready, Phys. Rev. Lett. 10, 342 (1963).

<sup>28</sup>C. M. Verber and A. H. Adelstein, J. Appl. Phys. 36, 1522 (1965).

<sup>29</sup>R. E. Honig and J. R. Woolston, Appl. Phys. Lett. 2, 138 (1963).

<sup>30</sup>J. F. Ready, Effects of High-Power Laser Radiation, Academic Press, New York, 1971 (Russ. Transl., Mir, M., 1974).

<sup>31</sup>J. F. Ready, Phys. Rev. 137, A620 (1965).

<sup>32</sup>W. L. Knecht, Appl. Phys. Lett. 8, 254 (1966).

<sup>33</sup>M. E. Marinchuk, Phys. Lett. A 34, 97 (1971).

<sup>34</sup>M. C. Teich and G. J. Wolga, Phys. Rev. 171, 809 (1968).

<sup>35</sup>M. C. Teich and G. J. Wolga, J. Opt. Soc. Am. 57, 542 (1967).

<sup>36</sup>P. Bloch, J. Appl. Phys. 35, 2052 (1964).

<sup>37</sup>N. V. Smith and W. E. Spicer, Phys. Rev. 188, 593 (1969).

<sup>38</sup>G. Farkas, I. Kertész, Z. Náray, and P. Varga, Phys. Lett. A 25, 572 (1967).

<sup>39</sup>E. M. Logothetis and P. L. Hartman, Phys. Rev. Lett. 18, 581 (1967).

<sup>40</sup>G. Farkas, I. Kertész, and Z. Náray, Phys. Lett. A 28, 190 (1968).

<sup>41</sup>M. Louis-Jacquet, C. R. Acad. Sci. Ser. B 273, 192 (1971).



- <sup>42</sup>L. I. Korshunov, V. A. Benderskiĭ, V. I. Gol'danskiĭ, and Ya. M. Zolotovitskiĭ, *Pis'ma Zh. Eksp. Teor. Fiz.* 7, 55 (1968) [*JETP Lett.* 7, 42 (1968)].
- <sup>43</sup>S. D. Babenko, V. A. Benderskiĭ, and T. S. Rudenko, *Pis'ma Zh. Eksp. Teor. Fiz.* 17, 71 (1973) [*JETP Lett.* 17, 48 (1973)].
- <sup>44</sup>S. D. Babenko, V. A. Benderskiĭ, A. G. Krivenko, and T. S. Rudenko, *Fiz. Tverd. Tela (Leningrad)* 16, 1337 (1974) [*Sov. Phys. Solid State* 16, 863 (1974)].
- <sup>45</sup>S. D. Babenko, V. A. Benderskiĭ, A. G. Krivenko, A. M. Brodskii, and G. I. Velichko, *Phys. Status Solidi (in press)*.
- <sup>46</sup>G. C. Barker, A. W. Gardner, and G. Bottura, *J. Electroanal. Chem.* 45, 21 (1973).
- <sup>47</sup>V. A. Benderskiĭ, S. D. Babenko, Ya. M. Zolotovitskiĭ, A. G. Krivenko, and T. S. Rudenko, *J. Electroanal. Chem.* 56, 325 (1974).
- <sup>48</sup>C. N. Berglund and W. E. Spicer, *Phys. Rev.* 136, A1030 (1964).
- <sup>49</sup>C. N. Berglund and W. E. Spicer, *Phys. Rev.* 136, A1044 (1964).
- <sup>50</sup>L. V. Keldysh, *Zh. Eksp. Teor. Fiz.* 47, 1945 (1964) [*Sov. Phys. JETP* 20, 1307 (1965)].
- <sup>51</sup>Y. Gontier and N. K. Rahman, *Lett. Nuovo Cimento* 9, 537 (1974).
- <sup>52</sup>S. Geltman and M. R. Teague, *J. Phys. B* 7, L22 (1974).
- <sup>53</sup>M. H. Mittleman, *Phys. Lett. A* 47, 55 (1974).
- <sup>54</sup>A. M. Brodskii and Yu. Ya. Gurevich, *Zh. Eksp. Teor. Fiz.* 60, 1452 (1971) [*Sov. Phys. JETP* 33, 786 (1971)].
- <sup>55</sup>N. G. Basov, M. M. Butslav, P. G. Kryukov, Yu. A. Matveets, E. A. Smirnova, B. M. Stepanov, S. D. Fanchenko, S. V. Chekalin, and R. V. Chikin, *Zh. Eksp. Teor. Fiz.* 65, 907 (1973) [*Sov. Phys. JETP* 38, 449 (1974)].
- <sup>56</sup>G. Farkas and Z. G. Horváth, Paper presented at Conf. on Laser and Its Applications, Dresden, 1970.
- <sup>57</sup>G. Farkas, Z. G. Horváth, and I. Kertész, and G. Kiss, *Lett. Nuovo Cimento* 1, 314 (1971).
- <sup>58</sup>G. Farkas, Z. G. Horváth, and I. Kertész, *Phys. Lett A* 39, 231 (1972).
- <sup>59</sup>G. Farkas and Z. G. Horváth, *Opt. Commun.* 12, 392 (1974).
- <sup>60</sup>G. Farkas, L. A. Lompre, and J. Thebault, Preprint D. Ph. 75.186, Saclay, France (1975).
- <sup>61</sup>K. Mitchell, *Proc. R. Soc. London Ser. A* 153, 513 (1936).
- <sup>62</sup>A. I. Baz', Ya. B. Zel'dovich, and A. M. Perelomov, *Rasseyanie, reaktsii i raspady v nerelativistskoĭ Kvantovoi mekhanike*, Nauka, M., 1971 (Scattering, Reactions, and Decay in Nonrelativistic Quantum Mechanics, Israel Program for Scientific Translations, Jerusalem, 1969).
- <sup>63</sup>G. Farkas, Z. G. Horváth, L. A. Lompre, and G. Petite, Abstracts of Papers presented at Second Conf. on Interaction of Electrons with Strong Electromagnetic Field, Budapest, (1975).
- <sup>64</sup>S. I. Anisimov, N. A. Inogamov, and Yu. V. Petrov, Abstracts of Papers presented at Second Conf. on Interaction of Electrons with Strong Electromagnetic Field, Budapest, 1975.
- <sup>65</sup>R. H. Fowler, *Phys. Rev.* 38, 45 (1931).
- <sup>66</sup>W. L. Schaich and N. W. Ashcroft, *Phys. Rev. B* 3, 2452 (1971).
- <sup>67</sup>G. D. Mahan, *Phys. Rev. Lett.* 24, 1068 (1970).
- <sup>68</sup>L. Sutton, *Phys. Rev. Lett.* 24, 386 (1970).
- <sup>69</sup>M. E. Marinichuk, *Izv. Akad. Nauk Mold. SSR* No. 12, 93 (1966).
- <sup>70</sup>I. I. Kantorovich, *Zh. Tekh. Fiz.* 47, 660 (1977). [*Sov. Phys. Tech. Phys.* 22, 397 (1977)].
- <sup>71</sup>A. Sommerfeld and H. A. Pethe, "Elektronentheorie der Metalle," in: *Handbuch der Physik*, Vol. 24, Part 2, Springer Verlag, Berlin, 1933, p. 333 (Russ. transl. GTTI, M.-L., 1933).
- <sup>72</sup>A. M. Perelomov and V. S. Popov, *Zh. Eksp. Teor. Fiz.* 54, 1799 (1968) [*Sov. Phys. JETP* 27, 967 (1968)].
- <sup>73</sup>A. I. Nikishov and V. I. Ritus, *Zh. Eksp. Teor. Fiz.* 52, 223 (1967) [*Sov. Phys. JETP* 25, 145 (1967)].
- <sup>74</sup>M. I. Kaganov, I. M. Lifshits, and L. V. Tanatarov, *Zh. Eksp. Teor. Fiz.* 31, 232 (1956) [*Sov. Phys. JETP* 4, 173 (1957)].
- <sup>75</sup>N. Kroó, Abstracts of Papers presented at Second Conf. on Interaction of Electrons with Strong Electromagnetic Field, Budapest, 1975.
- <sup>76</sup>I. Tamm and S. Shubin (Schubin), *Z. Phys.* 68, 97 (1931).
- <sup>77</sup>W. F. Krolkowski and W. E. Spicer, *Phys. Rev. B* 1, 478 (1970).
- <sup>78</sup>E. O. Kane, *Phys. Rev.* 147, 335 (1966).
- <sup>79</sup>S. W. Duckett, *Phys. Rev.* 166, 302 (1968).
- <sup>80</sup>G. D. Mahan, *Phys. Rev. B* 2, 4334 (1970).
- <sup>81</sup>A. M. Brodskii and A. V. Tsarevskii, *Zh. Eksp. Teor. Fiz.* 69, 936 (1975) [*Sov. Phys. JETP* 42, 476 (1975)].
- <sup>82</sup>M. Born and E. Wolf, *Principles of Optics*, 3rd ed., Pergamon Press, Oxford, 1965 (Russ. transl. Nauka, M., 1970).
- <sup>83</sup>P. O. Gartland, S. Berge, and B. J. Slagsvold, *Phys. Rev. Lett.* 30, 916 (1973).

Translated by A. Tybulewicz